RSC Advances

PAPER

Cite this: *RSC Adv.*, 2022, **12**, 11454

Synthesis, gene silencing activity, thermal stability, and serum stability of siRNA containing four (*S*)-5′-*C*-aminopropyl-2′-*O*-methylnucleosides (A, adenosine; U, uridine; G, guanosine; and C, cytidine)†

Ryohei Kajino,[a] Shuichi Sakamoto[e] and Yoshihito Ueno *[abcd]

Received 2nd February 2022
Accepted 30th March 2022

DOI: 10.1039/d2ra00705c

rsc.li/rsc-advances

Herein, we report the synthesis of (*S*)-5′-*C*-aminopropyl-2′-*O*-methyladenosine and (*S*)-5′-*C*-aminopropyl-2′-*O*-methylguanosine phosphoramidites and the properties of small interfering RNAs (siRNAs) containing four (*S*)-5′-*C*-aminopropyl-2′-*O*-methylnucleosides (A, adenosine; U, uridine; G, guanosine; and C, cytidine). The siRNAs containing (*S*)-5′-*C*-aminopropyl-nucleosides at the 3′- and 5′-regions of the passenger strand were well tolerated for RNA interference (RNAi) activity. Conversely, the (*S*)-5′-*C*-aminopropyl modification in the central region of the passenger strand decreased the RNAi activity. Furthermore, the siRNAs containing three or four consecutive (*S*)-5′-*C*-aminopropyl-2′-*O*-methylnucleosides at the 3′- and 5′-regions of the passenger strand exhibited RNAi activity similar to that of the corresponding 2′-*O*-methyl-modified siRNAs. Finally, it was observed that (*S*)-5′-*C*-aminopropyl modifications effectively improved the serum stability of the siRNAs, compared with 2′-*O*-methyl modifications. Therefore, (*S*)-5′-*C*-aminopropyl-2′-*O*-methylnucleosides would be useful for improving the serum stability of therapeutic siRNA molecules without affecting their RNAi activities.

Introduction

Small interfering RNA (siRNA) comprising double-strand RNA (dsRNA) triggers the degradation of complementary mRNA in a sequence-specific manner by mediated RNA interference (RNAi) machinery, which is a biological process in cells.[1–3] Accordingly, siRNAs possess potential as clinical tools for unmet medical needs. However, it is known that oligonucleotides such as siRNAs are degraded by nuclease inside and outside cells and are difficult to internalize into the cells, because they have negative charges over all the strands.[4,5] Chemical modifications such as 2′-*O*-methyl-RNA, 2′-fluoro-RNA, and phosphorothioate linkage enhance the cell membrane permeability of siRNAs and the stability of siRNAs toward nuclease.[6–11] In particular, chemically modified nucleosides are required for the clinical application of ligand-siRNA conjugates because this siRNA duplex is not protected from nucleolytic degradation.[12,13] To date, four siRNA drugs including patisiran, givosiran, lumasiran, and inclisiran, with 2′-*O*-methyl-, 2′-fluoro-, and phosphorothioate modifications have been approved by the Food and Drug Administration (FDA) and/or European Medicines Agency (EMA).

Recently, Manoharan *et al.* reported the synthesis and properties of C4′ and C5′-modified nucleosides, such as the 4′-*C*-methoxy-modified nucleosides, (*R*)-, or (*S*)-5′-*C*-methyl-modified nucleosides.[14–19] These nucleosides enhanced the nuclease resistance of oligonucleotides, compared with C2′-modified nucleosides without thermally destabilizing RNA duplexes and inhibiting gene silencing activity. Moreover, (*R*)- or (*S*)-5′-*C*-methylnucleosides improved the stability of oligonucleotides to snake venom phosphodiesterase (SVPD), compared with 4′-*C*-methoxy-nucleoside. This was due to the 5′-*C* modifications close to the phosphate linkages, compared with 4′-*C* modifications.[16] Recently, we reported the synthesis of RNA oligomers containing (*S*)-5′-*C*-aminopropyl-2′-*O*-methyluridine (**1**).[20] We observed that analog **1** significantly increased the stability of the RNAs in a buffer containing bovine serum and the binding affinity of the RNAs toward complementary RNA, compared with 4′-*C*-aminopropyl-2′-*O*-methyluridine and (*R*)-5′-*C*-aminopropyl-2′-*O*-methyluridine. The results suggested that

[a]United Graduate School of Agricultural Science, Gifu University, Japan. E-mail: uenoy@gifu-u.ac.jp; Fax: +81-58-293-2919; Tel: +81-58-293-2919

[b]Department of Life Science and Chemistry, The Graduate School of Natural Science and Technology, Gifu University, Japan

[c]Course of Applied Life Science, Faculty of Applied Biological Sciences, Gifu University, Japan

[d]Center for Highly Advanced Integration of Nano and Life Sciences (G-CHAIN), Gifu University, 1-1 Yanagido, Gifu, 501-1193, Japan

[e]Institute of Microbial Chemistry (BIKAKEN) Numazu Branch, Microbial Chemistry Research Foundation, 18-24 Miyamoto, Numazu, Shizuoka 410-0301, Japan

† Electronic supplementary information (ESI) available. See https://doi.org/10.1039/d2ra00705c

This article is licensed under a Creative Commons Attribution-NonCommercial 3.0 Unported Licence.

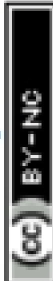

© 2022 The Author(s). Published by the Royal Society of Chemistry

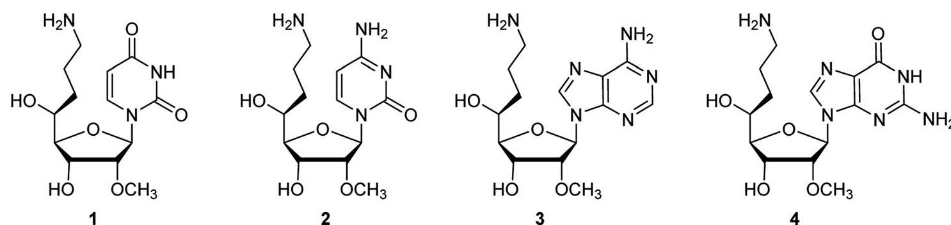

Fig. 1 Structures of (*S*)-5′-*C*-aminopropyl-2′-*O*-methyluridine[20] (**1**), (*S*)-5′-*C*-aminopropyl-2′-*O*-methylcytidine[21] (**2**), (*S*)-5′-*C*-aminopropyl-2′-*O*-methyladenosine (**3**), and (*S*)-5′-*C*-aminopropyl-2′-*O*-methylguanosine (**4**).

(*S*)-5′-*C*-aminopropyl-2′-*O*-methyl modifications were useful for oligonucleotide-based therapeutics.

Here, we synthesized the corresponding adenosine and guanosine analogs, (*S*)-5′-*C*-aminopropyl-2′-*O*-methyladenosine (**3**) and (*S*)-5′-*C*-aminopropyl-2′-*O*-methylguanosine (**4**). The properties of RNAs and siRNAs containing four (*S*)-5′-*C*-aminopropyl-2′-*O*-methylnucleosides (**1**, **2**, **3**, and **4**) were investigated in terms of thermal stability, serum stability, and the position-dependent effects of the analogs on the RNAi activity (Fig. 1).

Results and discussion

Synthesis of nucleoside analogs

The synthetic route of common synthetic intermediate **12** for the synthesis of the phosphoramidites of (*S*)-5′-*C*-aminopropyl-2′-*O*-methyladenosine (**3**) and (*S*)-5′-*C*-aminopropyl-2′-*O*-methylguanosine (**4**) is shown in Scheme 1. We used aldehyde derivative **5**, which was prepared according to a previously used procedure,[22] as a starting material. The allylation reaction of **5** using allyltrimethylsilane and boron trifluoride diethyl ether ($BF_3 \cdot OEt_2$)[23] afforded 5-*C*-allyl-ribofuranoside derivatives **6** and **7**. The configurations of the 5-carbons in **6** and **7** were determined by nuclear overhauser effect spectroscopy (NOESY).[21,24,25] To fix the conformations of the sugar moieties of **6** and **7**, the 3- and 5-hydroxy groups of **6** and **7** were protected by cyclic silyl groups. After removing the 3-*O*-*tert*-butyldiphenylsilyl (TBDPS) groups of **6** and **7**, the resulting 3, 5-dihydroxy derivatives were treated with 1,3-dichloro-1,1,3,3-tetraisopropyldisiloxane ($TIPDSCl_2$) in pyridine to afford 3,5-*O*-TIPDS derivatives **34** and **35** in 81% and 79% yields, respectively (Scheme 4). After the NOESY, a strong NOE was observed between the H-5 and H-3 of **35**, while no NOE was observed between the H-5 and H-3 of **34**. The results of the proton nuclear magnetic resonance (^{1}H NMR) measurement of **34** and **35** showed that the spin–spin coupling

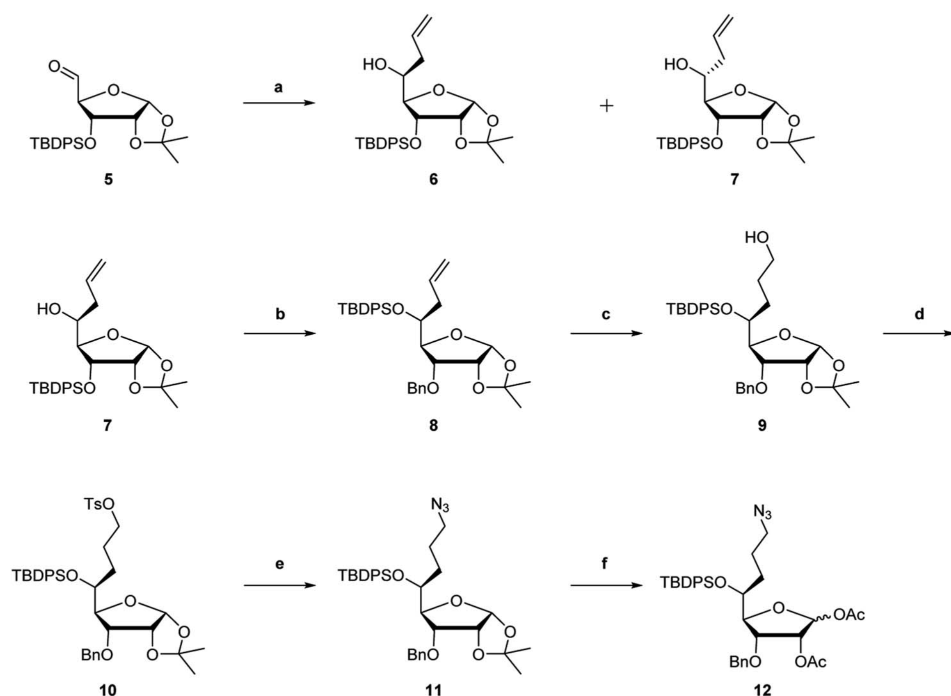

Scheme 1 Synthetic route of the common synthetic intermediate **12** for the synthesis of (*S*)-5′-*C*-aminopropyl-2′-*O*-methyladenosine and (*S*)-5′-*C*-aminopropyl-2′-*O*-methylguanosine phosphoramidite[a]. [a] Reagents and conditions: (a) allyltrimethylsilane, $BF_3 \cdot OEt_2$, CH_2Cl_2, −40 °C, 30 min, 82% (compounds **6** : **7** = 4 : 1); (b) BnBr, NaH, DMF, room temperature (rt), 16 h, 78%; (c) 9-BBN, THF, 30% H_2O_2 aq., 3 N NaOH aq., 40 °C, 1 h, 91%; (d) *p*-TsCl, pyridine, CH_2Cl_2, rt, 16 h, 95%; (e) NaN_3, DMF, 60 °C, 8 h, 90%; and (f) (i) 50% CF_3CO_2H aq., CH_2Cl_2, rt, 4.5 h and (ii) Ac_2O, pyridine, rt, 24 h, 81% (2 steps).

© 2022 The Author(s). Published by the Royal Society of Chemistry

constants between H-4 and H-5 of **34** and **35** were 2.0 and 8.0 Hz, respectively. The difference in the spin–spin coupling constants indicated that the conformations of H-4 and H-5 on the C4–C5 bond were *gauche*-form in **34** and *anti*-form in **35**, respectively. Thus, we concluded that the stereochemistry of C5 in ribofuranoside derivative **6** was an (*S*)-configuration, whereas that in ribofuranoside derivative **7** was an (*R*)-configuration. Next, we attempted to protect the 5-hydroxy function of **6** with a benzyl (Bn) group. It was revealed that the 3-*O*-TBDPS group migrated to the 5-hydroxy group of **6** when **6** was treated with sodium hydride (NaH).[26,27] Consequently, the benzylation reaction of **6** using NaH and benzyl bromide (BnBr) afforded the 5-*O*-TBDPS and 3-*O*-Bn derivative **8** in 78% yield. The hydroboration and oxidation of the allyl moiety of **8** produced the 5-*C*-hydroxypropyl-ribofuranose derivative **9** in 91% yield. The tosylation and azidation of the hydroxy function of **9** afforded the azidopropyl derivative **11** in a 50% yield from **9**. The deprotection of the isopropylidene moiety of **11** using 50% CF_3CO_2H in water, followed by the acetylation of 1,2-dihydroxyl groups using acetic anhydride (Ac_2O) in pyridine afforded a diastereomeric mixture of 1,2-diacetylated ribofuranoside **12** in 81% yield over two steps.

(*S*)-5′-*C*-aminopropyl-2′-*O*-methyladenosine phosphoramidite **22** was synthesized from the common synthetic intermediate **12** (Scheme 2). The stereoselective glycosylation of the 5-*C*-substituted ribofuranoside derivative **12** with N^6-benzoyl adenine using tin(IV) chloride ($SnCl_4$),[28,29] followed by deacetylation using potassium carbonate (K_2CO_3) in CH_3OH afforded a 2′-OH derivative **14**. The methylation of the 2′-OH moiety of **14** using CH_3I and NaH afforded the 2′-*O*-methyl derivative **15** in 72% yield. After removing the 5′-*O*-TBDPS and 3′-*O*-Bn groups in **15**, the resulting 5′,3′-dihydroxy nucleoside derivative was treated with TBDPSCl and imidazole in DMF to afford the 3′-*O*-TBDPS derivative **18** in 76% yield. The tritylation of the 5′-hydroxy function in **19** using dimethoxytrityl chloride (DMTrCl) successfully occurred in the presence of silver nitrate ($AgNO_3$). The reduction of the azide group in **19** by the Staudinger reaction, followed by the protection of the resulting amino function using ethyl trifluoroacetate (CF_3CO_2Et) afforded the fully protected adenosine derivative **20** in 93% yield. The deprotection of

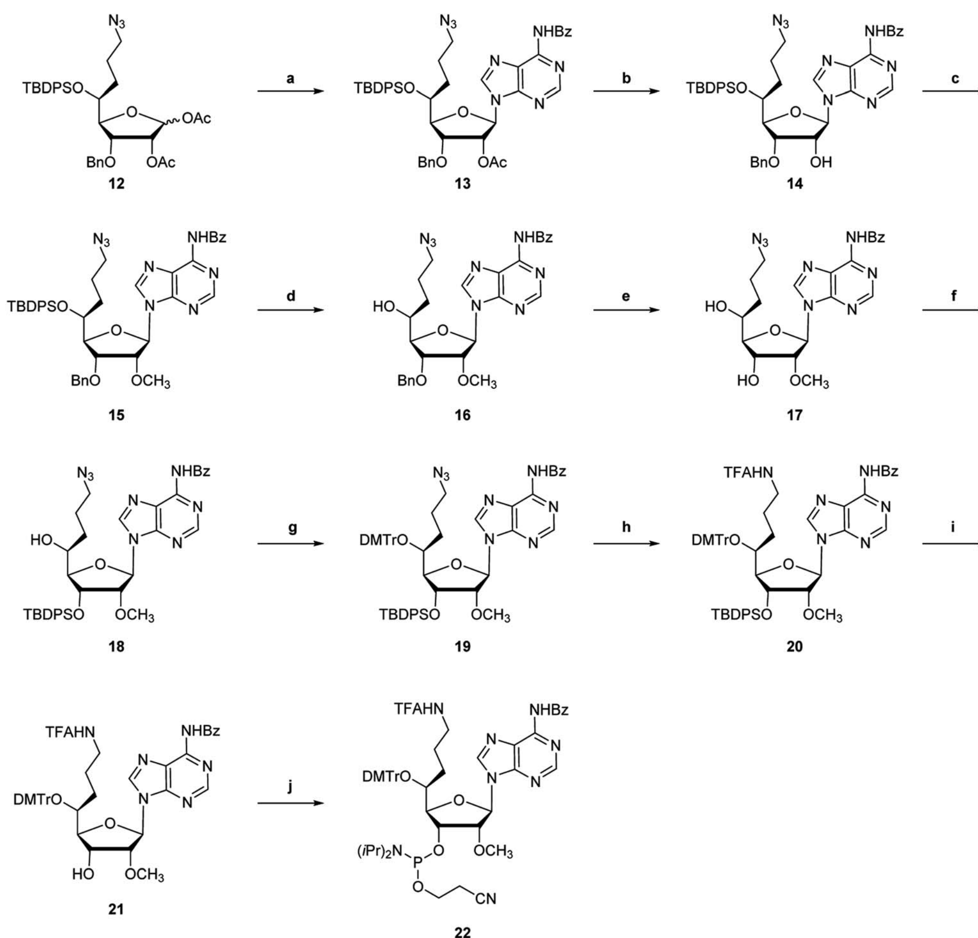

Scheme 2 Synthetic route of (*S*)-5′-*C*-aminopropyl-2′-*O*-methyladenosine phosphoramidite **22**[a]. [a] Reagents and conditions: (a) N^6-benzoyl adenine, $SnCl_4/CH_2Cl_2$, CH_3CN, rt, 2 h, 70%; (b) K_2CO_3, CH_3OH, 0 °C, 30 min, 92%; (c) CH_3I, NaH, THF, 0 °C, 2.5 h, 72%; (d) TBAF/THF, THF, rt, 16 h, 92%; (e) BCl_3/CH_2Cl_2, CH_2Cl_2, −78 °C, 2 h, 89%; (f) TBDPSCl, imidazole, DMF, rt, 24 h, 76%; (g) DMTrCl, $AgNO_3$, pyridine, THF, 40 °C, 12 h, 72%; (h) (i) Ph_3P, H_2O, THF, 45 °C, 12 h and (ii) CF_3CO_2Et, Et_3N, CH_2Cl_2, rt, 24 h, 93%; (i) TBAF/THF, THF, rt, 24 h, 99%; and (j) 2-cyanoethyl-*N*,*N*-diisopropylchlorophosphoramidite, DIPEA, THF, rt, 1 h, 80%.

 © 2022 The Author(s). Published by the Royal Society of Chemistry

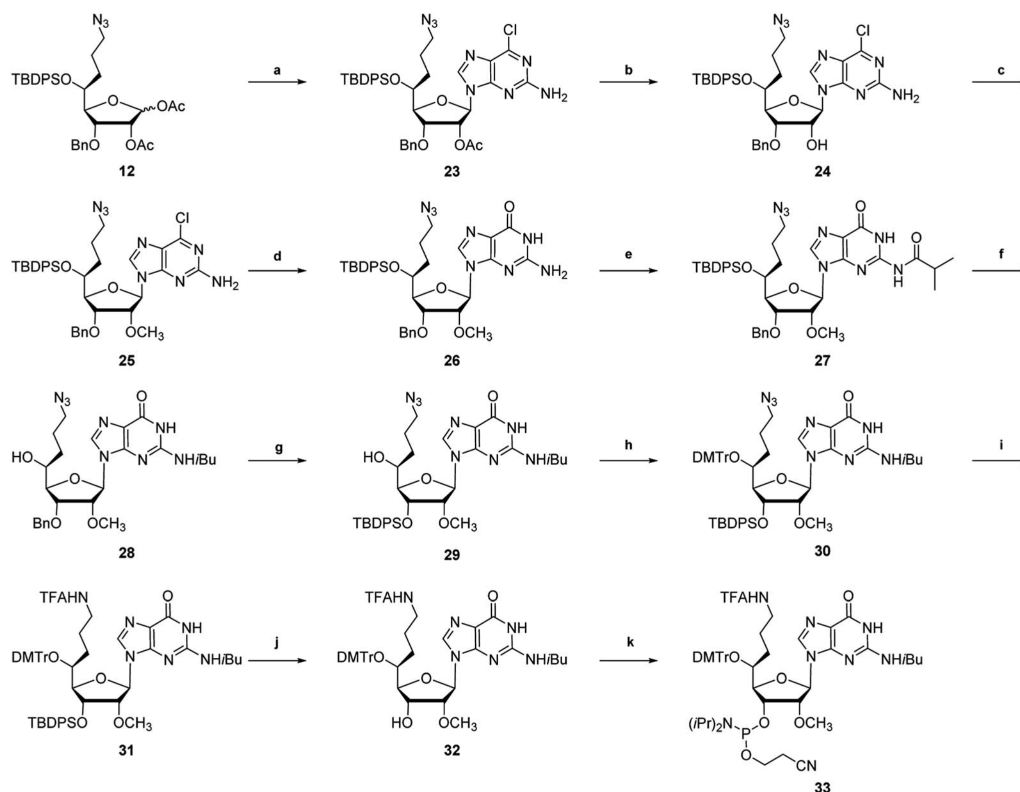

Scheme 3 Synthetic route of (*S*)-5′-*C*-aminopropyl-2′-*O*-methylguanosine phosphoramidite **33**[a]. [a] Reagents and conditions: (a) 2-amino-6-chloropurine, *N*,*O*-bis(trimethylsilyl)acetamide, TMSOTf, toluene, 80 °C, 15 h, 75%; (b) K_2CO_3, CH_3OH, 0 °C, 30 min, 93%; (c) CH_3I, NaH, DMF, 0 °C, 7 h, 69%; (d) 3-hydroxypropionitrile, NaH, THF, 0 °C, 6 h, 85%; (e) isobutyric anhydride, DMAP, DMF, 60 °C, 13 h, 77%; (f) TBAF/THF, THF, rt, 46 h, 83% (g) (i) BCl_3/CH_2Cl_2, CH_2Cl_2, −78 °C, 4 h; (ii) TBDPSCl, imidazole, DMF, 0 °C, 29 h, 50% (2 steps); (h) DMTrCl, $AgNO_3$, pyridine, THF, 40 °C, 12 h, 92%; (i) (i) Ph_3P, H_2O, THF, 45 °C, 22 h and (ii) CF_3CO_2Et, Et_3N, CH_2Cl_2, rt, 19 h, 77% (2 steps); (j) TBAF/THF, THF, rt, 24 h, 70%; and (k) 2-cyanoethyl-*N*,*N*-diisopropylchlorophosphoramidite, DIPEA, THF, rt, 1 h, 73%.

the 3′-*O*-silyl group in **20** by treatment with *n*-tetrabutylammonium fluoride (TBAF) afforded **21** in 99% yield. Finally, the 3′-hydroxy function of nucleoside **21** was phosphorylated by treatment with 2-cyanoethyl-*N*,*N*-diisopropylchlorophosphoramidite (CEP-Cl) to afford (*S*)-5′-*C*-aminopropyl-2′-*O*-methyladenosine phosphoramidite **22** in 80% yield.

The synthetic route of (*S*)-5′-*C*-aminopropyl-2′-*O*-methylguanosine phosphoramidite is shown in Scheme 3. Diacetate **12** was glycosylated by treatment with the silylated 2-amino-6-chloropurine and trimethylsilyl triflate (TMSOTf)[30] to afford nucleoside derivative **23** in 75% yield. Compound **23** was treated with K_2CO_3 in CH_3OH, followed by the methylation of the resulting 2′-hydroxyl function of **24** by treatment with CH_3I and NaH to afford the 2′-*O*-methylnucleoside derivative **25**. The substitution reaction of the chlorine atom at the 6-position of the 2-amino-6-chloropurine moiety of **25** with a hydroxyl group successfully proceeded by treatment with 3-hydroxypropionitrile and NaH to afford the guanosine derivative **26** in 85% yield. Thereafter, the exocyclic amino function of **26** was protected with the isobutyryl (iBu) group to afford the protected guanosine derivative **27** in 77% yield. Similar to the synthesis of the (*S*)-5′-*C*-aminopropyl-2′-*O*-methyladenosine phosphoramidite, **22**, **27** was converted into the corresponding phosphoramidite **33**.

Oligonucleotide synthesis

The nucleoside analogs **3** and **4** were incorporated into oligonucleotides using phosphoramidites **22** and **33** with a DNA/RNA synthesizer. RNA phosphoramidites and 2′-*O*-methyl-modified phosphoramidites were prepared as 0.10 M solutions in CH_3CN. (*S*)-5′-*C*-aminopropyl-2′-*O*-methyl-modified phosphoramidites were prepared as 0.15 M solutions in CH_3CN. 5-Benzylthio-1*H*-tetrazole as 0.25 M solution in CH_3CN was used as activator. The coupling time used for all phosphoramidites was 12 min. In this condition, the coupling efficiency of (*S*)-5′-*C*-aminopropyl-2′-*O*-methyl-modified phosphoramidites was nearly equal to that of RNA phosphoramidites. After the synthesis, to prevent the additional reaction of acrylonitrile with the 5′-*C*-aminopropyl functional groups, the controlled-pore glass (CPG) beads were treated with 10% diethylamine in CH_3CN at room temperature for 5 min and with concentrated NH_3/40% methylamine (1 : 1, v/v) solution at 65 °C for 10 min. The 2′-*O*-TBDMS groups were removed by treatment with $Et_3N \cdot 3HF$ in dimethyl sulfoxide (DMSO) at 65 °C for 1.5 h. RNAs were purified using 20% denaturing polyacrylamide gel electrophoresis (PAGE). The RNA sequences synthesized in this study are listed in Tables 1–4 and S1–S7.†

© 2022 The Author(s). Published by the Royal Society of Chemistry

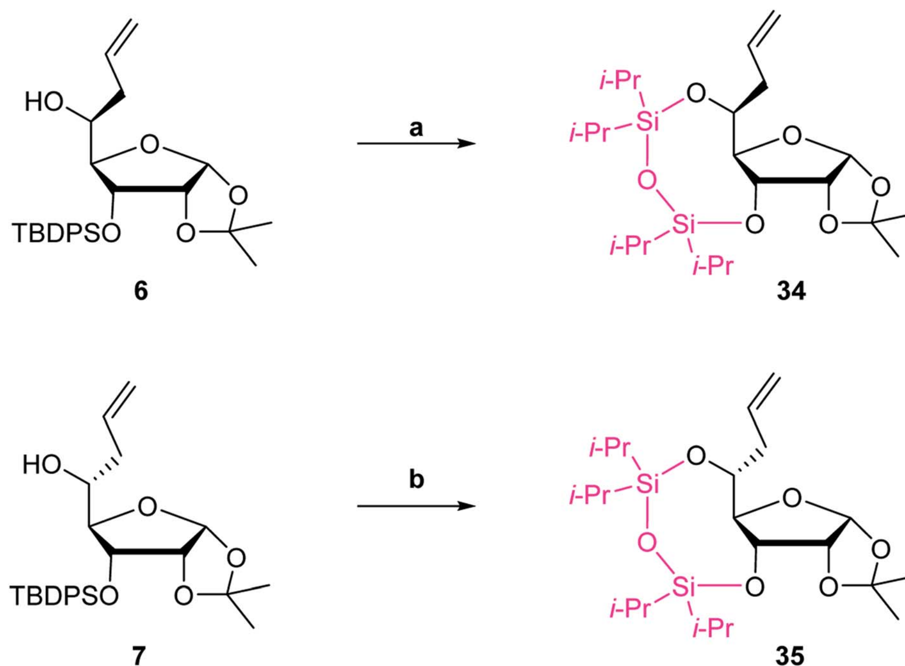

Scheme 4 Synthetic route of 3-, 5-*O*-TIPDS derivatives **34** and **35**[a]. [a] Reagents and conditions: (a) (i) TBAF/THF, THF, rt, 3.5 h and (ii) $TIPDSCl_2$, pyridine, rt, 21 h, 81% (2 steps) and (b) (i) TBAF/THF, THF, rt, 1 h and (ii) $TIPDSCl_2$, pyridine, rt, 21 h, 79% (2 steps).

Thermal stability of siRNA duplexes

We evaluated the effect of (*S*)-5′-*C*-aminopropyl modifications on the thermal stability of siRNAs (siRNA **1–15**). Temperature-induced melting was investigated by ultraviolet (UV) spectroscopy in 10 mM sodium phosphate buffer (pH of 7.0) containing 100 mM NaCl. The melting temperature (T_m) values are listed in Tables 1–4. As shown in Tables 1–3, the T_m values of the 2′-*O*-methyl-modified siRNAs (siRNA **2**, **4**, **6**, **8**, **10**, **12**, and

Table 1 Sequences of ssRNAs, siRNAs, and T_m values of siRNAs

Abbreviation of siRNA	Abbreviation of ssRNA	Passenger strand (5'-3') [a] / Guide strand (3'-5')	T_m (°C) [b]	ΔT_m (°C) [c]
siRNA 1	RNA 1	5′-GGCCUUUCACUACUCCUACUU-3′	77.9 (±0.1)	–
	RNA 8	3'-UUCCGGAAAGUGAUGAGGAUG-5'		
siRNA 2	RNA 2	5'-GGCCUUUCACUACUCCUACUU-3'	77.4 (±0.1)	–
	RNA 8	3'-UUCCGGAAAGUGAUGAGGAUG-5'		
siRNA 3	RNA 3	5'-GGCCUUUCACUACUCCUACUU-3'	75.7 (±0.3)	–1.7 (±0.2)
	RNA 8	3'-UUCCGGAAAGUGAUGAGGAUG-5'		
siRNA 4	RNA 4	5'-GGCCUUUCACUACUCCUACUU-3'	77.4 (±0.3)	–
	RNA 8	3'-UUCCGGAAAGUGAUGAGGAUG-5'		
siRNA 5	RNA 5	5'-GGCCUUUCACUACUCCUACUU-3'	73.3 (±0.2)	–4.1 (±0.1)
	RNA 8	3'-UUCCGGAAAGUGAUGAGGAUG-5'		
siRNA 6	RNA 6	5'-GGCCUUUCACUACUCCUACUU-3'	77.7 (±0.2)	–
	RNA 8	3'-UUCCGGAAAGUGAUGAGGAUG-5'		
siRNA 7	RNA 7	5'-GGCCUUUCACUACUCCUACUU-3'	75.2 (±0.1)	–2.5 (±0.2)
	RNA 8	3'-UUCCGGAAAGUGAUGAGGAUG-5'		

[a] Blue and red letters denote 2′-*O*-methylnucleosides and (*S*)-5′-*C*-aminopropyl-2′-*O*-methylnucleosides, respectively. [b] The T_m values were determined using 3 μM dsRNA in a buffer containing 10 mM sodium phosphate (pH of 7.0) and 100 mM NaCl. All experiments were performed thrice, and data are presented as the mean ± SD. [c] ΔT_m represents [T_m (siRNA$_{(S)\text{-}5'\text{-}C\text{-aminopropyl-}2'\text{-}O\text{-methyl}}$) − T_m (siRNA$_{2'\text{-}O\text{-methyl}}$)].

 © 2022 The Author(s). Published by the Royal Society of Chemistry

Table 2 Sequences of ssRNAs, siRNAs, and T_m values of siRNAs

Abbreviation of siRNA	Abbreviation of ssRNA	Passenger strand (5'-3') [a] Guide strand (3'-5')	T_m (°C) [b]	ΔT_m (°C) [c]
siRNA 1	RNA 1	5′-GGCCUUUCACUACUCCUACUU-3′	77.9 (±0.1)	–
	RNA 8	3'-UUCCGGAAAGUGAUGAGGAUG-5'		
siRNA 8	RNA 9	5'-GGCCUUUCA**CUA**CUCCUACUU-3'	77.6 (±0.1)	–
	RNA 8	3'-UUCCGGAAAGUGAUGAGGAUG-5'		
siRNA 9	RNA 10	5'-GGCCUUUCA**CUA**CUCCUACUU-3'	73.9 (±0.2)	–3.7 (±0.1)
	RNA 8	3'-UUCCGGAAAGUGAUGAGGAUG-5'		
siRNA 10	RNA 11	5'-GGCCUU**UCA**CUACUCCUACUU-3'	77.4 (±0.2)	–
	RNA 8	3'-UUCCGGAAAGUGAUGAGGAUG-5'		
siRNA 11	RNA 12	5'-GGCCUU**UCA**CUACUCCUACUU-3'	74.1 (±0.2)	–3.3 (±0.1)
	RNA 8	3'-UUCCGGAAAGUGAUGAGGAUG-5'		
siRNA 12	RNA 13	5'-GGC**CUU**UCACUACUCCUACUU-3'	77.8 (±0.03)	–
	RNA 8	3'-UUCCGGAAAGUGAUGAGGAUG-5'		
siRNA 13	RNA 14	5'-GGC**CUU**UCACUACUCCUACUU-3'	75.1 (±0.2)	–2.7 (±0.2)
	RNA 8	3'-UUCCGGAAAGUGAUGAGGAUG-5'		

[a] Blue and red letters denote 2′-*O*-methylnucleosides and (*S*)-5′-*C*-aminopropyl-2-*O*-methylnucleosides, respectively. [b] The T_m values were determined using 3 μM dsRNA in a buffer containing 10 mM sodium phosphate (pH of 7.0) and 100 mM NaCl. All experiments were performed thrice, and data are presented as the mean ± SD. [c] ΔT_m represents [T_m (siRNA$_{(S)\text{-}5'\text{-}C\text{-aminopropyl-}2'\text{-}O\text{-methyl}}$) − T_m (siRNA$_{2'\text{-}O\text{-methyl}}$)].

14) were siRNA **2**, 77.4 °C; siRNA **4**, 77.4 °C; siRNA **6**, 77.7 °C; siRNA **8**, 77.6 °C; siRNA **10**, 77.4 °C; siRNA **12**, 77.8 °C; and siRNA **14**, 77.9 °C, respectively. Those of the (*S*)-5′-*C*-aminopropyl-2′-*O*-methyl-modified siRNAs (siRNA **3**, **5**, **7**, **9**, **11**, **13**, and **15**) were siRNA **3**, 75.7 °C; siRNA **5**, 73.3 °C; siRNA **7**, 75.2 °C; siRNA **9**, 73.9 °C; siRNA **11**, 74.1 °C; siRNA **13**, 75.1 °C; and siRNA **15**, 78.0 °C, respectively. Therefore, the ΔT_m [T_m (siRNA$_{(S)\text{-}5'\text{-}C\text{-aminopropyl-}2'\text{-}O\text{-methyl}}$) − T_m (dsRNA$_{2'\text{-}O\text{-methyl}}$)] values of siRNAs **3**, **5**, **7**, **9**, **11**, **13**, and **15** were calculated to be −1.7, −4.1, −2.5, −3.7, −3.3, −2.7, and 0.0 °C, respectively. These results suggested that the (*S*)-5′-*C*-aminopropyl-2′-*O*-methyl modification at the passenger strand decreased the thermal stability of the siRNA duplex compared to the 2′-*O*-methyl modification, except for the modification of the 5′-end of the passenger strand.

Next, we measured the T_m of the siRNAs containing 2′-*O*-methylnucleosides or (*S*)-5′-*C*-aminopropyl-2′-*O*-methylnucleosides at the 3′- and 5′-regions of the passenger strand (siRNA **16**–**21**). As shown in Table 4, the T_m values of the 2′-*O*-methyl-modified siRNAs (siRNA **16**, **18**, and **20**) were siRNA **16**, 77.6 °C; siRNA **18**, 77.6 °C; siRNA **20**, 78.6 °C, respectively. Those of the (*S*)-5′-*C*-aminopropyl-2′-*O*-methyl-modified siRNAs (siRNAs **17**, **19**, and **21**) were siRNA **17**, 76.3 °C; siRNA **19**, 76.0 °C; and siRNA **21**, 72.6 °C, respectively. The ΔT_m [T_m (siRNA$_{(S)\text{-}5'\text{-}C\text{-}}$

Table 3 Sequences of ssRNAs, siRNAs, and T_m values of siRNAs

Abbreviation of siRNA	Abbreviation of ssRNA	Passenger strand (5'-3') [a] Guide strand (3'-5')	T_m (°C) [b]	ΔT_m (°C) [c]
siRNA 1	RNA 1	5′-GGCCUUUCACUACUCCUACUU-3'	78.0 (±0.1)	–
	RNA 8	3'-UUCCGGAAAGUGAUGAGGAUG-5'		
siRNA 14	RNA 15	5'-**GGC**CUUUCACUACUCCUACUU-3'	77.9 (±0.1)	–
	RNA 8	3'-UUCCGGAAAGUGAUGAGGAUG-5'		
siRNA 15	RNA 16	5'-**GGC**CUUUCACUACUCCUACUU-3'	78.0 (±0.1)	0.0 (±0.03)
	RNA 8	3'-UUCCGGAAAGUGAUGAGGAUG-5'		

[a] Blue and red letters denote 2′-*O*-methylnucleosides and (*S*)-5′-*C*-aminopropyl-2′-*O*-methylnucleosides, respectively. [b] The T_m values were determined using 3 μM dsRNA in a buffer containing 10 mM sodium phosphate (pH of 7.0) and 100 mM NaCl. All experiments were performed thrice, and data are presented as the mean ± SD. [c] ΔT_m represents [T_m (siRNA$_{(S)\text{-}5'\text{-}C\text{-aminopropyl-}2'\text{-}O\text{-methyl}}$) − T_m (siRNA$_{2'\text{-}O\text{-methyl}}$)].

© 2022 The Author(s). Published by the Royal Society of Chemistry

Table 4 Sequences of ssRNAs, siRNAs, and T_m values of siRNAs

Abbreviation of siRNA	Abbreviation of ssRNA	Passenger strand (5'-3') [a] Guide strand (3'-5')	T_m (°C) [b]	ΔT_m (°C) [c]
siRNA 1	RNA 1	5′-GGCCUUUCACUACUCCUACUU-3′	77.4 (±0.1)	–
	RNA 8	3'-UUCCGGAAAGUGAUGAGGAUG-5'		
siRNA 16	RNA 17	5'-GGCCUUUCACUACUCCUACUU-3'	77.6 (±0.2)	–
	RNA 8	3'-UUCCGGAAAGUGAUGAGGAUG-5'		
siRNA 17	RNA 18	5'-GGCCUUUCACUACUCCUACUU-3'	76.3 (±0.1)	–1.3 (±0.2)
	RNA 8	3'-UUCCGGAAAGUGAUGAGGAUG-5'		
siRNA 18	RNA 19	5'-GGCCUUUCACUACUCCUACUU-3'	77.6 (±0.0)	-
	RNA 8	3'-UUCCGGAAAGUGAUGAGGAUG-5'		
siRNA 19	RNA 20	5'-GGCCUUUCACUACUCCUACUU-3'	76.0 (±0.2)	–1.6 (±0.1)
	RNA 8	3'-UUCCGGAAAGUGAUGAGGAUG-5'		
siRNA 20	RNA 21	5'-GGCCUUUCACUACUCCUACUU-3'	78.6 (±0.2)	-
	RNA 8	3'-UUCCGGAAAGUGAUGAGGAUG-5'		
siRNA 21	RNA 22	5'-GGCCUUUCACUACUCCUACUU-3'	72.6 (±0.3)	–6.0 (±0.2)
	RNA 8	3'-UUCCGGAAAGUGAUGAGGAUG-5'		

[a] Blue and red letters denote 2′-*O*-methylnucleosides and (*S*)-5′-*C*-aminopropyl-2-*O*-methylnucleosides, respectively. [b] The T_m values were determined using 3 μM dsRNA in a buffer containing 10 mM sodium phosphate (pH of 7.0) and 100 mM NaCl. All experiments were performed thrice, and data are presented as the mean ± SD. [c] ΔT_m represents [T_m (siRNA$_{(S)\text{-}5'\text{-}C\text{-aminopropyl-}2'\text{-}O\text{-methyl}}$) − T_m (siRNA$_{2'\text{-}O\text{-methyl}}$)].

aminopropyl-2′-*O*-methyl) − T_m (dsRNA$_{2'\text{-}O\text{-methyl}}$)] values of siRNAs **17**, **19**, and **21** were calculated as −1.3, −1.6 and −6.0 °C, respectively. Previously, we reported that the incorporation of eight (*S*)-5′-*C*-aminopropyl-2′-*O*-methyluridines in the passenger strand of an siRNA resulted in a change in T_m of −0.8 °C/modification, compared with that in the unmodified siRNA.[20] Oppositely, the change in the T_m of siRNA **19** containing eight (*S*)-5′-*C*-aminopropyl-2′-*O*-methylnucleosides was −0.18 °C/modification. These results suggested that the thermal stability of siRNAs can be improved by the consecutive introduction of the analogs.

RNAi activity

We evaluated the RNAi activity of the 2′-*O*-methyl-modified, (*S*)-5′-*C*-aminopropyl-modified, and unmodified siRNAs by a dual-luciferase reporter assay using HeLa cells, in which the target luciferase genes were constitutively expressed. All the siRNAs targeted the *Renilla* luciferase genes, while the expression of firefly luciferase genes was used as a control. The HeLa cells were transfected with the siRNAs using RNAiMAX, and the expression of both luciferase genes was analyzed after 24 h of incubation. The relative percentages of *Renilla* and firefly

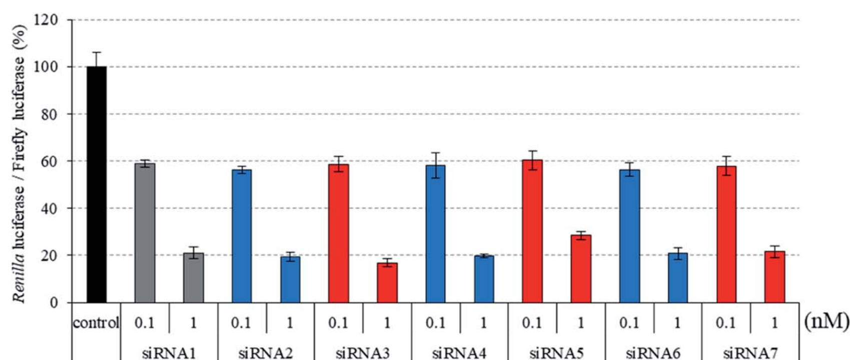

Fig. 2 RNAi activity of siRNAs modified by three consecutive analogs at the passenger strand. siRNAs were transfected into HeLa cells at concentrations of 0.1 and 1 nM. After a 24 h incubation, the activities of *Renilla* and firefly luciferases in the cells were determined using the dual-luciferase reporter assay system. The results were confirmed by at least three independent transfection experiments with two cultures each and are expressed as the average of four experiments as the mean ± SD.

 © 2022 The Author(s). Published by the Royal Society of Chemistry

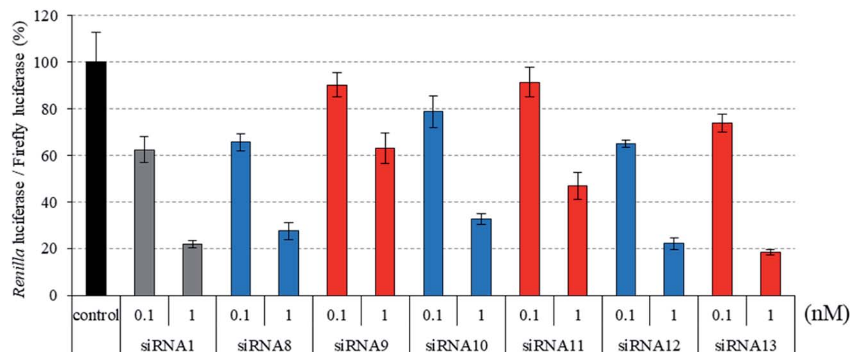

Fig. 3 RNAi activity of siRNAs modified by three consecutive analogs at the passenger strand. siRNAs were transfected into HeLa cells at concentrations of 0.1 and 1 nM. After a 24 h incubation, the activities of *Renilla* and firefly luciferases in the cells were determined using the dual-luciferase reporter assay system. The results were confirmed by at least three independent transfection experiments with two cultures each and are expressed as the average of four experiments as the mean ± SD.

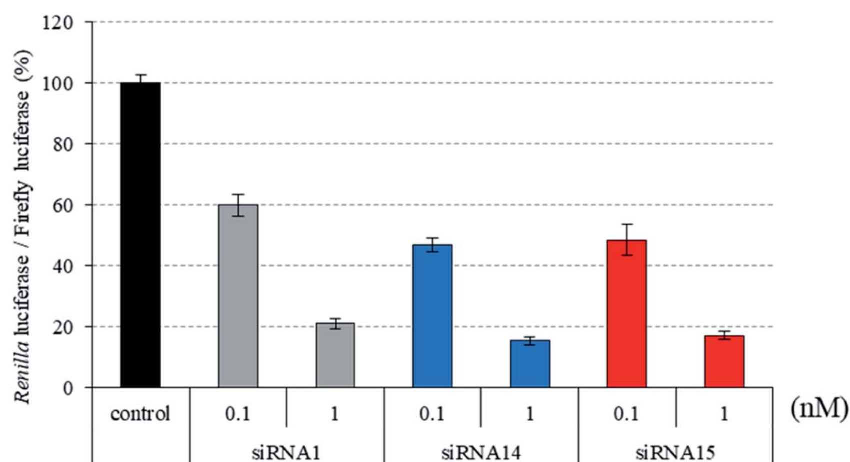

Fig. 4 RNAi activity of siRNAs modified by three consecutive analogs at the passenger strand. siRNAs were transfected into HeLa cells at concentrations of 0.1 and 1 nM. After a 24 h incubation, the activities of *Renilla* and firefly luciferases in the cells were determined using the dual-luciferase reporter assay system. The results were confirmed by at least three independent transfection experiments with two cultures each and are expressed as the average of four experiments as the mean ± SD.

luciferase activities, compared with the controls containing no siRNAs are shown in Fig. 2–7, Tables 5, 6, and S1–S6.†

Recently, we reported that siRNAs containing (*S*)-5′-*C*-aminopropyl-2′-*O*-methyluridines at the passenger strand down-regulated the expression of the target *Renilla* luciferase gene with equal or slightly lower activity, compared with the unmodified siRNA. Here, we investigated the position-dependent effects of (*S*)-5′-*C*-aminopropyl modifications on the RNAi activity of siRNAs. First, we synthesized modified siRNAs (siRNAs **2–15**), which contained three (*S*)-5′-*C*-aminopropyl-2′-*O*-methylnucleosides or three 2′-*O*-methylnucleosides in succession at every position of the passenger strand. As shown in Fig. 2–4, siRNAs **3**, **5**, **7**, **13**, and **15**, which contain three consecutive (*S*)-5′-*C*-aminopropyl-nucleosides at the 3′- or 5′-regions of the passenger strand, repressed the expression of the *Renilla* luciferase gene with activities similar to those of the corresponding 2′-*O*-methyl-modified siRNAs **2**, **4**, **6**, **12**, and **14** and the unmodified siRNA **1** at concentrations of 0.1 and 1 nM. Oppositely, the incorporation of three consecutive (*S*)-5′-*C*-aminopropyl-nucleosides at the central regions of the passenger strand decreased the silencing activities of siRNAs **9** and **11**, compared with the corresponding 2′-*O*-methyl-modified siRNAs **8** and **10** and the unmodified siRNA **1** at concentrations of 0.1 and 1 nM (Fig. 2). The introduction of (*S*)-5′-*C*-aminopropyl-nucleosides at the 3′- or 5′-regions of the passenger strand was well tolerated for eliciting RNAi activity, and the incorporation of (*S*)-5′-*C*-aminopropyl-nucleosides at the central regions of the passenger strand decreased the gene silencing activity of the siRNAs. When argonaute-2 and siRNA formed the RNA-induced silencing complex (RISC) in cells, the passenger strand of siRNA was hydrolyzed by the slicer activity of the P-element-induced wimpy testis (PIWI) domain of argonaute-2.[31,32] Therefore, it was suggested that siRNAs **9** and **11** were prevented from the hydrolysis of the passenger strand because of the (*S*)-5′-*C*-aminopropyl modification near the cleavage site. The results showed that siRNAs containing (*S*)-5′-*C*-aminopropyl-nucleosides at the 3′- or 5′-regions of the

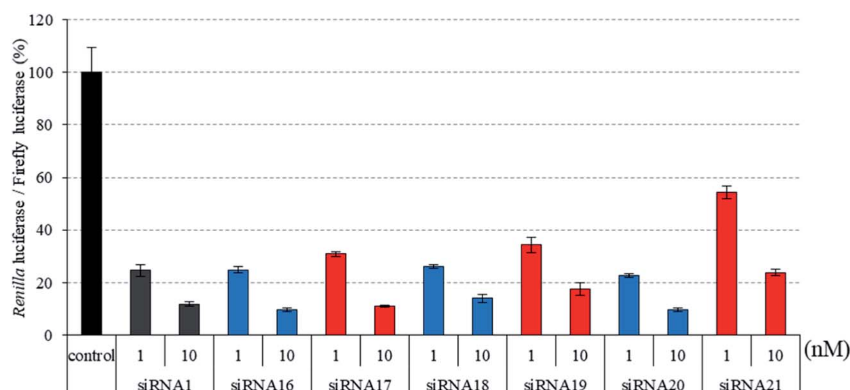

Fig. 5 RNAi activity of siRNAs modified by three, four, or five consecutive analogs at the 3′- and 5′-regions of the passenger strand. siRNAs were transfected into HeLa cells at concentrations of 1 and 10 nM. After a 24 h incubation, the activities of *Renilla* and firefly luciferases in the cells were determined using the dual-luciferase reporter assay system. The results were confirmed by at least three independent transfection experiments with two cultures each and are expressed as the average of four experiments as the mean ± SD.

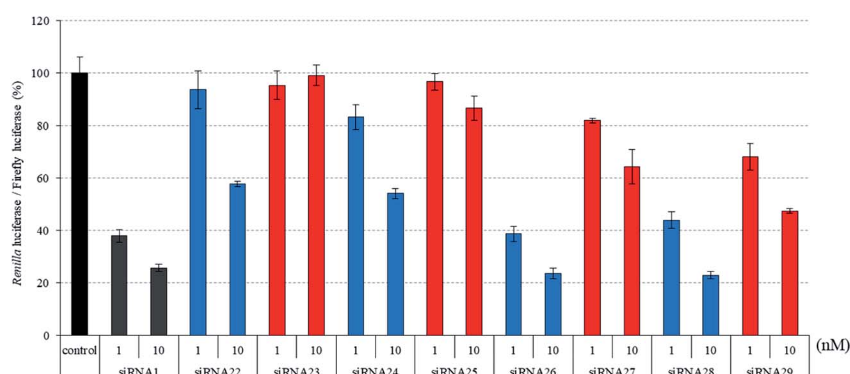

Fig. 6 RNAi activity of siRNA modified by analogs at the guide strand. siRNAs were transfected into HeLa cells at concentrations of 1 and 10 nM. After a 24 h incubation, the activities of *Renilla* and firefly luciferases in the cells were determined using the dual-luciferase reporter assay system. The results were confirmed by at least three independent transfection experiments with two cultures each and are expressed as the average of four experiments as the mean ± SD.

passenger strand could efficiently suppress the expression of the target gene.

Next, we assessed the silencing activity of siRNAs (siRNA **16**–**21**) containing three, four, or five consecutive analogs at the 3′- and 5′-regions of the passenger strand. As shown in Fig. 5, the RNAi activities of siRNAs **17** and **19**, which contained three and four consecutive analogs at the 3′- and 5′-regions, respectively, were equal to or slightly lower than those of the corresponding

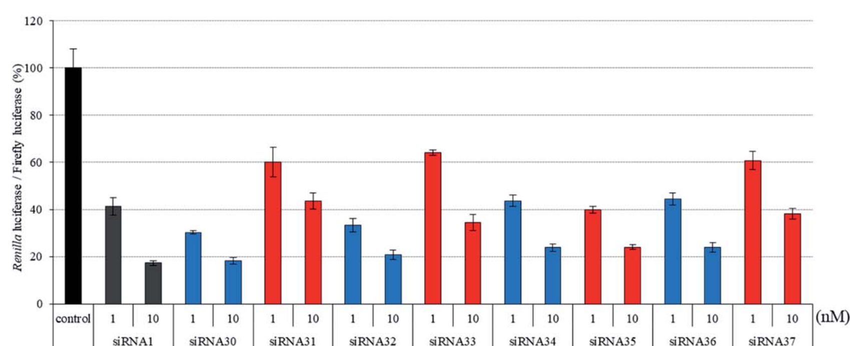

Fig. 7 RNAi activity of siRNAs modified by analogs at the guide strand. siRNAs were transfected into HeLa cells at concentrations of 1 and 10 nM. After a 24 h incubation, the activities of *Renilla* and firefly luciferases in the cells were determined using a dual-luciferase reporter assay system. The results were confirmed by at least three independent transfection experiments with two cultures each and are expressed as the average of four experiments as the mean ± SD.

 © 2022 The Author(s). Published by the Royal Society of Chemistry

Table 5 Sequences of ssRNAs and siRNAs used for RNAi activity study

Abbreviation of siRNA	Abbreviation of ssRNA	sequence [a]
siRNA 1	RNA 1	5'-GGCCUUUCACUACUCCUACUU-3'
	RNA 8	3'-UUCCGGAAAGUGAUGAGGAUG-5'
siRNA 22	RNA 1	5'-GGCCUUUCACUACUCCUACUU-3'
	RNA 23	3'-UUCCGGAAAGUGAUGAGGAUG-5'
siRNA 23	RNA 1	5'-GGCCUUUCACUACUCCUACUU-3'
	RNA 24	3'-UUCCGGAAAGUGAUGAGGAUG-5'
siRNA 24	RNA 1	5'-GGCCUUUCACUACUCCUACUU-3'
	RNA 25	3'-UUCCGGAAAGUGAUGAGGAUG-5'
siRNA 25	RNA 1	5'-GGCCUUUCACUACUCCUACUU-3'
	RNA 26	3'-UUCCGGAAAGUGAUGAGGAUG-5'
siRNA 26	RNA 1	5'-GGCCUUUCACUACUCCUACUU-3'
	RNA 27	3'-UUCCGGAAAGUGAUGAGGAUG-5'
siRNA 27	RNA 1	5'-GGCCUUUCACUACUCCUACUU-3'
	RNA 28	3'-UUCCGGAAAGUGAUGAGGAUG-5'
siRNA 28	RNA 1	5'-GGCCUUUCACUACUCCUACUU-3'
	RNA 29	3'-UUCCGGAAAGUGAUGAGGAUG-5'
siRNA 29	RNA 1	5'-GGCCUUUCACUACUCCUACUU-3'
	RNA 30	3'-UUCCGGAAAGUGAUGAGGAUG-5'

[a] Blue and red letters denote 2′-*O*-methylnucleosides and (*S*)-5′-*C*-aminopropyl-2-*O*-methylnucleosides, respectively.

2′-*O*-methyl-modified siRNAs **16** and **18**, whereas that of siRNA **21** containing five consecutive analogs was lower than that of the corresponding 2′-*O*-methyl-modified siRNA **20**. These results suggested that the simultaneous incorporation of (*S*)-5′-*C*-aminopropyl-nucleosides at the 3′- and 5′-regions of the passenger strand was tolerable for eliciting RNAi activity. However, it was observed that increasing the number of contiguous analogs in the 3′- and 5′-regions of the passenger strand tended to further reduce RNAi activity.

To investigate the position-dependent effects of (*S*)-5′-*C*-aminopropyl modifications in the seed region of the siRNA, we synthesized siRNAs containing one (*S*)-5′-*C*-aminopropyl-nucleoside at positions 1–8 from the 5′-end of the guide strand and evaluated their silencing activity. It was found that the thermal stability of these siRNA duplexes containing one (*S*)-5′-*C*-aminopropyl-nucleoside at the guide strand were similar to those of the corresponding 2′-*O*-methyl-modified siRNA duplexes (Fig. S5–S7 and Tables S7–S9†). As shown in Fig. 6, incorporation of (*S*)-5′-*C*-aminopropyl-nucleoside at positions 1

© 2022 The Author(s). Published by the Royal Society of Chemistry

Table 6 Sequences of ssRNAs and siRNAs used for RNAi activity study

Abbreviation of siRNA	Abbreviation of ssRNA	sequence [a]
siRNA 1	RNA 1	5'-GGCCUUUCACUACUCCUACUU-3'
	RNA 8	3'-UUCCGGAAAGUGAUGAGGAUG-5'
siRNA 30	RNA 1	5'-GGCCUUUCACUACUCCUACUU-3'
	RNA 31	3'-UUCCGGAAAGUGAUGAGGAUG-5'
siRNA 31	RNA 1	5'-GGCCUUUCACUACUCCUACUU-3'
	RNA 32	3'-UUCCGGAAAGUGAUGAGGAUG-5'
siRNA 32	RNA 1	5'-GGCCUUUCACUACUCCUACUU-3'
	RNA 33	3'-UUCCGGAAAGUGAUGAGGAUG-5'
siRNA 33	RNA 1	5'-GGCCUUUCACUACUCCUACUU-3'
	RNA 34	3'-UUCCGGAAAGUGAUGAGGAUG-5'
siRNA 34	RNA 1	5'-GGCCUUUCACUACUCCUACUU-3'
	RNA 35	3'-UUCCGGAAAGUGAUGAGGAUG-5'
siRNA 35	RNA 1	5'-GGCCUUUCACUACUCCUACUU-3'
	RNA 36	3'-UUCCGGAAAGUGAUGAGGAUG-5'
siRNA 36	RNA 1	5'-GGCCUUUCACUACUCCUACUU-3'
	RNA 37	3'-UUCCGGAAAGUGAUGAGGAUG-5'
siRNA 37	RNA 1	5'-GGCCUUUCACUACUCCUACUU-3'
	RNA 38	3'-UUCCGGAAAGUGAUGAGGAUG-5'

[a] Blue and red letters denote 2′-*O*-methylnucleosides and (*S*)-5′-*C*-aminopropyl-2′-*O*-methylnucleosides, respectively.

or 2 was detrimental to the RNAi activity of the siRNAs. Pradeepkumar and Harikrishna reported that the 5′-phosphates of positions 1 and 2 in the guide strand of siRNA interacted with many amino acid residues, such as T526, Y529, Q545, Q548, K550, N551, K566, K570, and R814.[33] Thus, it was considered that the (*S*)-5′-*C*-aminopropyl modification incorporated at the 5′-end of the guide strand disturbed the important interaction between the guide strand and argonaute-2 protein to form RISC. As shown in Fig. 6 and 7, incorporating the (*S*)-5′-*C*-aminopropyl-nucleoside at positions 3, 4, 5, 6, or 8 tended to decrease the RNAi activity of the siRNAs, compared with that of the 2′-*O*-methyl modification. However, the (*S*)-5′-*C*-aminopropyl-modification at position 7 from the 5′-end of the guide strand was well tolerated for RNAi activity. Therefore, to understand why the (*S*)-5′-*C*-aminopropyl modification at position 7 of the guide strand was well tolerated for the RNAi activity of siRNA, we performed a modeling study on the interaction between argonaute-2 and the (*S*)-5′-*C*-aminopropyl modification in siRNA. As shown in Fig. S8,† a pocket on the protein surface that can accommodate the aminopropyl side-chain existed near position 7 from the 5′-end of the guide strand. Thus, it was considered that the RNAi activity of siRNA **35** containing the

 © 2022 The Author(s). Published by the Royal Society of Chemistry

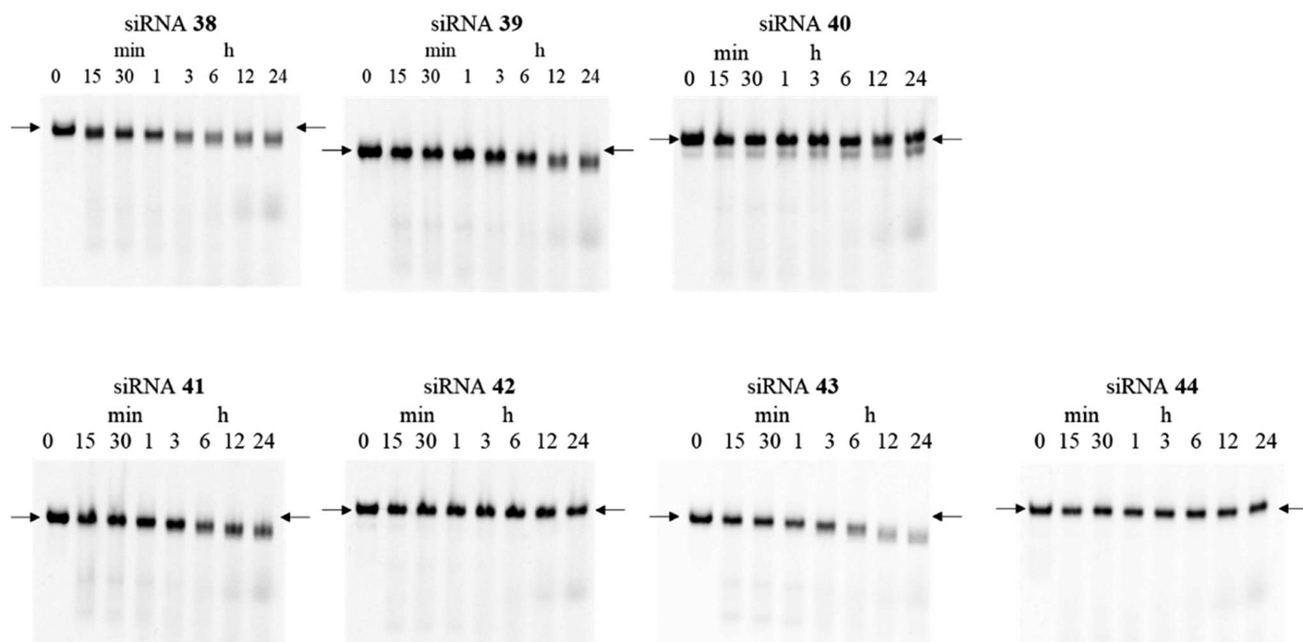

Fig. 8 Polyacrylamide gel electrophoresis (PAGE) analysis donated stability of siRNA (4.5 μM) in 50% bovine serum. Fluorescein-labeled siRNAs **38–44** (600 pmol) were incubated in a buffer containing 50% bovine serum. Subsequently, the reaction mixtures at various incubation times (0, 15, and 30 min and 1, 3, 6, 12, and 24 h) were analyzed by nondenaturing PAGE. Arrows refer to the full-length band of the siRNAs.

analog at position 7 was retained by accommodating the aminopropyl side chain in the pocket on the argonaute-2 protein.

Serum stability

Chemical modifications such as 2′-*O*-methyl-RNA and 2′-fluoro-RNA are essential for siRNA-based therapeutics because unmodified siRNAs are rapidly degraded by nucleases in serum. Thus, to investigate the effects of (*S*)-5′-*C*-aminopropyl modifications at the 3′- and 5′-regions of the passenger strand on the serum stability of the siRNAs, we assessed the stability of the modified siRNAs in a buffer containing bovine serum. Chemical modifications at the guide strand of siRNA are important for achieving serum stability. Considering that the introduction of the (*S*)-5′-*C*-aminopropyl modification at the guide strand decreased the RNAi activity of siRNAs by disturbing the interaction with the argonaute-2 protein, we used siRNAs comprising the guide strand containing phosphorothioate, 2′-*O*-methyl, and 2′-fluoro modifications in this study. The fluorescein-labeled siRNAs **38–44** (Table 7) were incubated in a buffer containing 50% bovine serum, and the reaction mixtures at various incubation times (0, 15, and 30 min and 1, 3, 6, 12, and 24 h) were analyzed by PAGE.

As shown in Fig. 8, when the (*S*)-5′-*C*-aminopropyl-modified siRNAs **40**, **42**, and **44** were used, the bands corresponding to

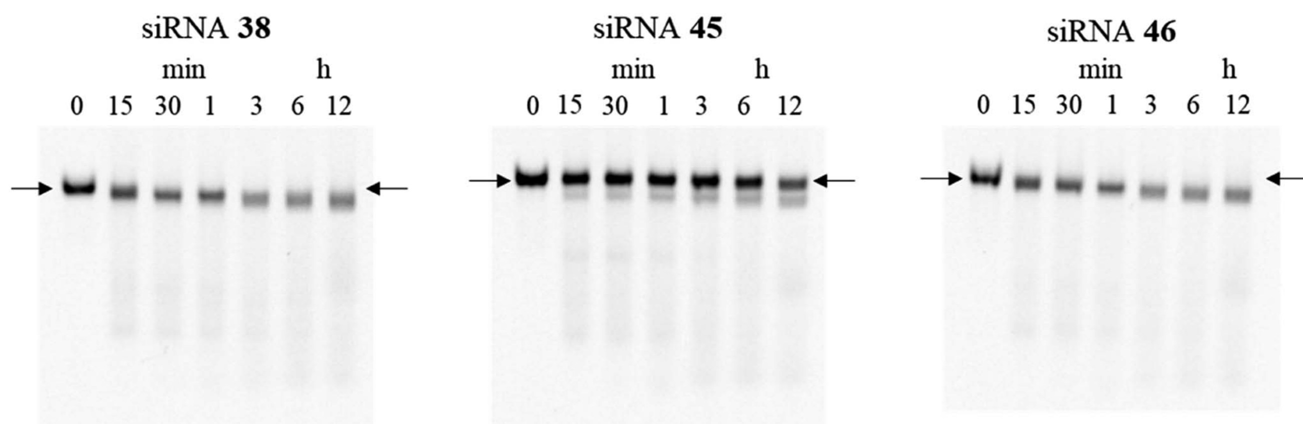

Fig. 9 Polyacrylamide gel electrophoresis (PAGE) analysis donated stability of siRNA (4.5 μM) in 50% bovine serum. Fluorescein-labeled siRNAs **38**, **45**, and **46** (600 pmol) were incubated in a buffer containing 50% bovine serum. Subsequently, the reaction mixtures at various incubation times (0, 15, and 30 min and 1, 3, 6, and 12 h) were analyzed by nondenaturing PAGE. Arrows refer to the full-length band of the siRNAs.

© 2022 The Author(s). Published by the Royal Society of Chemistry

the full-length of the siRNAs remained intact even after 24 h of incubation. With the unmodified siRNA **38** or the 2′-*O*-methyl-modified siRNAs **39**, **41**, and **43**, it was observed that the bands corresponding to the full-length of the siRNAs gradually degraded and became faint. Thus, it was observed that the (*S*)-5′-*C*-aminopropyl modifications enhanced the serum stability of the siRNA, compared with the 2′-*O*-methyl modifications.

Furthermore, to investigate the effect of the site-specific incorporation of the (*S*)-5′-*C*-aminopropyl modifications on serum stability, we evaluated the stability of siRNAs **45** and **46** containing three consecutive (*S*)-5′-*C*-aminopropyl-nucleosides at the 3′- or 5′-regions of the passenger strand in 50% bovine serum. As shown in Fig. 9, when siRNA **45** with three consecutive (*S*)-5′-*C*-aminopropyl-nucleosides at the 3′-region was used, the band corresponding to the full-length siRNA remained intact even after 12 h of incubation, whereas with siRNA **46** with three consecutive (*S*)-5′-*C*-aminopropyl-nucleosides at the 5′-region, the band corresponding to the full-length siRNA gradually degraded and became faint. These results indicated that incorporating the (*S*)-5′-*C*-aminopropyl modification at the 3′-region of siRNA effectively improved the resistance toward the nuclease in serum, compared with that of the analog at the 5′-

Table 7 Sequences of ssRNAs and siRNAs for serum stability test

Abbreviation of siRNA	Abbreviation of ssRNA	sequence[a]
siRNA 38	RNA 1	5'-GGCCUUUCACUACUCCUACUU-3'
	RNA 39	3'-U^U^C^C^GGAAAGUGAUGAGGAUG-5'-F
siRNA 39	RNA 17	5'-GGCCUUUCACUACUCCUACUU-3'
	RNA 23	3'-U^U^C^C^GGAAAGUGAUGAGGAUG-5'-F
siRNA 40	RNA 18	5'-GGCCUUUCACUACUCCUACUU-3'
	RNA 39	3'-U^U^C^C^GGAAAGUGAUGAGGAUG-5'-F
siRNA 41	RNA 19	5'-GGCCUUUCACUACUCCUACUU-3'
	RNA 39	3'-U^U^C^C^GGAAAGUGAUGAGGAUG-5'-F
siRNA 42	RNA 20	5'-GGCCUUUCACUACUCCUACUU-3'
	RNA 39	3'-U^U^C^C^GGAAAGUGAUGAGGAUG-5'-F
siRNA 43	RNA 21	5'-GGCCUUUCACUACUCCUACUU-3'
	RNA 39	3'-U^U^C^C^GGAAAGUGAUGAGGAUG-5'-F
siRNA 44	RNA 22	5'-GGCCUUUCACUACUCCUACUU-3'
	RNA 39	3'-U^U^C^C^GGAAAGUGAUGAGGAUG-5'-F
siRNA 45	RNA 3	5'-GGCCUUUCACUACUCCUACUU-3'
	RNA 39	3'-U^U^C^C^GGAAAGUGAUGAGGAUG-5'-F
siRNA 46	RNA 16	5'-GGCCUUUCACUACUCCUACUU-3'
	RNA 39	3'-U^U^C^C^GGAAAGUGAUGAGGAUG-5'-F

[a] F, blue letters, green letters, red letters, and ^ denote fluorescein, 2′-*O*-methylnucleosides, 2′-fluoro-nucleosides, (*S*)-5′-*C*-aminopropyl-2′-*O*-methylnucleosides, and phosphorothioate linkages, respectively.

 © 2022 The Author(s). Published by the Royal Society of Chemistry

Table 8 Sequences of ssRNAs and siRNAs for RT-qPCR analysis

Abbreviation of siRNA	Abbreviation of ssRNA	Sense (Passenger) strand[a] Antisense (Guide) strand[a]
siRNA 47 (siGL3)	RNA 40	5'-CUUACGCUGAGUACUUCGATT-3'
	RNA 41	3'-TTGAAUGCGACUCAUGAAGCU-5'
siRNA 48	RNA 42	5'-UAGUCAACUUGGUAUAUUUTT-3'
	RNA 43	3'-TTAUCAGUUGAACCAUAUAAA-5'
siRNA 49	RNA 44	5'-UAGUCAACUUGGUAUAUUU^T^T-3'
	RNA 45	3'-T^T^A^U^C^AGUUGAACCAUAUAAA-5'

[a] Blue letters, red letters, and ^ denote 2′-*O*-methylnucleosides, (*S*)-5′-*C*-aminopropyl-2′-*O*-methylnucleosides, and phosphorothioate linkages, respectively.

region of siRNA. Previously, Gait *et al.* reported that siRNA degradation in serum occurred similar to RNase A-like mechanism, cleaving at UpA sequences close to the end of each strand in the siRNA.[34] siRNA **38** used in this study contains the UpA sequence at the 3′-end region of the passenger strand. The siRNAs were considered to be degraded at the UpA site in bovine serum. siRNAs **42** and **44** contained the (*S*)-5′-*C*-aminopropyl-uridine analog instead of the U of the UpA site; therefore, they were hardly degraded. Thus, the incorporation of the (*S*)-5′-*C*-aminopropyl modification at the most vulnerable degradation site of siRNA such as the UpA sequence near the 3′-end region of the strands would be useful for improving the biological stability of siRNAs in mammalian serum.

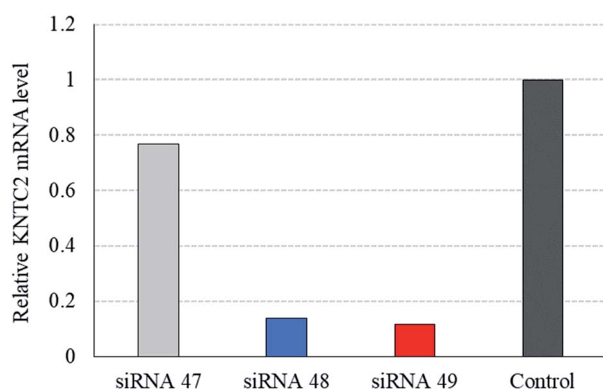

Fig. 10 RNAi activity of *KNTC2* siRNA modified by (*S*)-5′-*C*-aminopropyl-2′-*O*-methylnucleosides. siRNAs targeting *KNTC2* gene (siRNA **48**, siRNA **49**) or firefly luciferase gene (siRNA **47**) were transfected to HCT116 cells at a concentration of 10 nM. After a 24 hours incubation, cells were replated in fresh cell culture media and were further incubated for another 24 hours. Then, total RNA of the cells was extracted and *KNTC2* mRNA levels were determined by RT-qPCR. Data were normalized to the level of *ACTB* mRNA and are presented as relative mRNA levels compared to the un-transfected control group (control). Data represent the mean of two independent experiments.

Quantitative reverse-transcriptional PCR (RT-qPCR) analysis

We also examined the effect of the (*S*)-5′-*C*-aminopropyl modifications on RNAi activity in another siRNA targeting human *KNTC2* gene, which is considered to be a therapeutic target for several cancers.[35,36] We synthesized a modified *KNTC2*-siRNA (siRNA **49**) which contained four (*S*)-5′-*C*-aminopropyl methyl-uridines at the 3′-regions of the passenger strand (Table 8) and investigated its RNAi activity on the *KNTC2* mRNA level in human colon cancer HCT116 cells (Fig. 10). A quantitative reverse-transcriptional PCR (RT-qPCR) analysis revealed that the RNAi activity of the (*S*)-5′-*C*-aminopropyl modified siRNA (siRNA **49**) was nearly equal to that of the corresponding 2′-*O*-methyl-modified *KNTC2*-siRNA (siRNA **48**). This result supports our mention that the simultaneous incorporation of (*S*)-5′-*C*-aminopropyl-nucleosides at the 3′-regions of the passenger strand was tolerable for eliciting RNAi activity.

Conclusion

Here, we successfully synthesized (*S*)-5′-*C*-aminopropyl-2′-*O*-methyladenosine phosphoramidite (**22**) and (*S*)-5′-*C*-amino-propyl-2′-*O*-methylguanosine phosphoramidite (**33**). It was observed that the introduction of (*S*)-5′-*C*-aminopropyl-nucleosides at the 3′- and/or 5′-regions of the passenger strand of siRNA was tolerable for the RNAi activity of the siRNAs, whereas the incorporation of analogs at the central region of the passenger strand of siRNA was detrimental to the RNAi activity. Furthermore, the (*S*)-5′-*C*-aminopropyl modifications at the passenger strand thermally destabilized siRNA duplexes, compared with the corresponding 2′-*O*-methyl modifications, except for the consecutive incorporation of the (*S*)-5′-*C*-amino-propyl modifications at the 5′-region of the passenger strand. Finally, it was revealed that the incorporation of the (*S*)-5′-*C*-aminopropyl modifications at the vulnerable degradation sites of siRNA effectively enhanced the serum stability of siRNA. Therefore, incorporating the (*S*)-5′-*C*-aminopropyl-2′-*O*-

© 2022 The Author(s). Published by the Royal Society of Chemistry

methylnucleosides into appropriate sites of siRNAs would be useful for improving the serum stability of therapeutic siRNA molecules without affecting their RNAi activities.

Experimental section

General remark

All chemicals and dry solvents (THF, DMF, CH_2Cl_2, CH_3CN, toluene and pyridine) were obtained from commercial sources and used without any further purification. Thin layer chromatography (TLC) was performed on silica gel plates precoated with fluorescent indicator with visualization by UV light or by dipping into a solution of 5% (v/v) concentrated H_2SO_4 in mixture of *p*-anisaldehyde and methanol and then heating. Silica gel (63–210 mesh) was used for column chromatography. ^{1}H NMR (400 or 600 MHz), ^{13}C {^{1}H}NMR (101 or 151 MHz), ^{31}P NMR (162 MHz) were recorded on 400 or 600 MHz NMR equipment. $CDCl_3$ or DMSO-d_6 was used as a solvent for obtaining NMR spectra. Chemical shifts (δ) are given in parts per million (ppm) from $CDCl_3$ (7.26 ppm), DMSO-d_6 (2.50 ppm) for ^{1}H NMR spectra and from $CDCl_3$ (77.2 ppm) DMSO-d_6 (39.5 ppm) for ^{13}C {^{1}H}NMR spectra. The abbreviations s, d, t, q, and m signify singlet, doublet, triplet, quadruplet, and multiplet, respectively. High resolution mass spectra (HRMS) were obtained in positive ion electrospray ionization (ESI-TOF) mode.

Experimental procedures

(*S*)-5-*C*-Allyl-1,2-*O*-isopropylidene-3-*O*-[(1,1-dimethylethyl) diphenylsilyl]-α-D-ribose (6) and (*S*)-5-*C*-allyl-1,2-*O*-isopropylidene-3-*O*-[(1,1-dimethylethyl)diphenylsilyl]-α-D-ribose (7). To a solution of **5** in CH_2Cl_2 (50 mL) cooled to −40 °C was added $BF_3 \cdot OEt_2$ (1.27 mL, 10.12 mmol), allyltrimethylsirane (1.28 mL, 8.09 mmol) under argon atmosphere. After 30 min at −40 °C, the reaction mixture was quenched with saturated $NaHCO_3$ aqueous. The organic layer was washed with saturated $NaHCO_3$ aqueous and brine, dried (Na_2SO_4). After concentration, the residue was purified by a silica gel column chromatography (hexane : EtOAc = 5 : 1) to afford product as a colorless oil (1.94 g, 4.14 mmol, 82%, *S* : *R* = 4 : 1). Compound **6**: ^{1}H NMR (400 MHz, $CDCl_3$): δ 7.78–7.76 (m, 2H), 7.71–7.69 (m, 2H), 7.47–7.35 (m, 6H), 5.89–5.78 (m, 1H), 5.53 (d, *J* = 3.6 Hz, 1H), 5.14–5.11 (m, 2H), 4.08 (dd, *J* = 8.6, 4.0 Hz, 1H), 3.99 (dd, *J* = 8.8, 1.2 Hz, 1H), 3.94 (t, *J* = 4.0 Hz, 1H), 3.69–3.64 (m, 1H), 2.41–2.32 (m, 2H), 1.56 (s, 3H), 1.50 (d, *J* = 8.4 Hz, 1H), 1.23 (s, 3H), 1.10 (s, 9H); ^{13}C {^{1}H}NMR (151 MHz, $CDCl_3$): δ 136.2, 136.0, 134.8, 133.7, 133.5, 130.1, 130.0, 127.9, 127.6, 117.8, 112.7, 104.0, 81.4, 79.2, 72.7, 68.3, 39.6, 27.1, 27.0, 26.5, 19.5; HRMS (ESI-TOF) *m*/*z*: $[M + Na]^+$ calcd for $C_{27}H_{36}NaO_5Si$ 491.2230, found 491.2229.

Compound **7**: ^{1}H NMR (400 MHz, $CDCl_3$): δ 7.79–7.71 (m, 4H), 7.47–7.34 (m, 6H), 5.88–5.77 (m, 1H), 5.47 (d, *J* = 3.6 Hz, 1H), 5.11–5.07 (m, 2H), 4.10–4.09 (m, 2H), 3.89–3.84 (m, 1H), 3.79–3.77 (m, 1H), 2.31–2.27 (m, 2H), 1.98 (d, *J* = 3.6 Hz, 1H), 1.54 (s, 3H), 1.14 (s, 3H), 1.10 (s, 9H); ^{13}C {^{1}H}NMR (151 MHz, $CDCl_3$): δ 136.4, 136.1, 135.0, 133.7, 133.4, 130.1, 130.0, 127.9, 127.5, 117.8, 112.5, 103.4, 81.4, 79.1, 73.5, 70.6, 36.8, 27.1, 26.9, 26.3, 19.5; HRMS (ESI-TOF) *m*/*z*: $[M + Na]^+$ calcd for $C_{27}H_{36}NaO_5Si$ 491.2230, found 491.2223.

(*S*)-5-*C*-Allyl-3-*O*-benzyl-5-*O*-[(1,1-dimethylethyl)diphenylsilyl]-1,2-*O*-isopropylidene-α-D-ribose (8). To a solution of **6** (1.00 g, 2.13 mmol) in DMF (10 mL) was added NaH (0.17 g, 4.25 mmol) under argon atmosphere. After 30 min, to a reaction mixture was added BnBr (0.50 mL, 4.25 mmol) at 0 °C, stirred for 16 h at room temperature. After the reaction mixture was quenched with CH_3OH, the mixture was washed with saturated $NaHCO_3$ aqueous and brine, dried (Na_2SO_4). After concentration, the residue was purified by a silica gel column chromatography (hexane : EtOAc = 15 : 1) to afford desired product **8** as a colorless oil (0.92 g, 1.65 mmol, 78%). ^{1}H NMR (600 MHz, $CDCl_3$): δ 7.72–7.69 (m, 4H), 7.43–7.28 (m, 11H), 5.80 (d, *J* = 3.6 Hz, 1H), 5.52–5.45 (m, 1H), 4.87–4.82 (m, 2H), 4.65 (d, *J* = 11.4 Hz, 1H), 4.56 (t, *J* = 3.0 Hz, 1H), 4.38 (d, *J* = 12.0 Hz, 1H), 4.10 (dd, *J* = 9.0, 1.8 Hz, 1H), 4.02 (dd, *J* = 8.4, 4.2 Hz, 1H), 3.92 (ddd, *J* = 9.6, 4.8, 1.8 Hz, 1H), 1.53 (s, 3H), 1.37 (s, 3H), 1.00 (s, 9H); ^{13}C {^{1}H}NMR (151 MHz, $CDCl_3$): δ 138.0, 136.1, 136.0, 134.4, 134.1, 133.9, 129.8, 129.7, 128.5, 128.1, 127.9, 127.7, 127.6, 117.8, 113.2, 104.5, 80.2, 78.2, 78.1, 72.1, 71.9, 38.7, 27.2, 27.1, 19.6; HRMS (ESI-TOF) *m*/*z*: $[M + Na]^+$ calcd for $C_{34}H_{42}NaO_5Si$ 581.2699, found 581.2677.

3-*O*-Benzyl-(*S*)-5-*C*-hydroxypropyl-5-*O*-[(1,1-dimethylethyl) diphenylsilyl]-1,2-*O*-isopropylidene-α-D-ribose (9). Under argon atmosphere, 9-borabicyclo[3.3.1]nonane (9-BBN, 0.5 M in THF, 9.50 mL) was added dropwise to a solution of compound **8** (0.92 g, 1.65 mmol) in THF (16 mL) and stirred for 13 h at room temperature. Water was added to the reaction mixture until evolution of gas ceased. 3 N NaOH solution (3.6 mL) was added, and then, slowly 30% aqueous hydrogen peroxide solution (1.87 mL) was added while keeping the temperature between 40 °C. The mixture was stirred and extracted with water and ethyl acetate. The organic layer was washed with neutral phosphate buffer solution and brine, dried over Na_2SO_4, filtered, and concentrated. The crude material was purified by column chromatography (33% ethyl acetate in hexane) to afford desired product **9** as a white solid (0.86 g, 1.50 mmol, 91%). ^{1}H NMR (600 MHz, $CDCl_3$): δ 7.72–7.69 (m, 4H), 7.43–7.29 (m, 11H), 5.77 (d, *J* = 3.6 Hz, 1H), 4.68 (d, *J* = 10.8 Hz, 1H), 4.57 (t, *J* = 3.6 Hz, 1H), 4.38 (d, *J* = 12.0 Hz, 1H), 4.11 (dd, *J* = 8.4, 2.4 Hz, 1H), 3.96 (dd, *J* = 8.7, 4.8 Hz, 1H), 3.93–3.90 (m, 1H), 3.30–3.27 (m, 2H), 1.70–1.63 (m, 2H), 1.56 (s, 3H), 1.44–1.39 (m, 2H), 1.37 (s, 3H), 1.02 (s, 9H), 0.98 (bs, 1H); ^{13}C {^{1}H}NMR (151 MHz, $CDCl_3$): δ 137.9, 136.1, 134.4, 134.0, 129.8, 129.7, 128.5, 128.1, 128.0, 127.7, 127.6, 113.0, 104.4, 80.7, 78.2, 78.0, 72.1, 72.1, 62.7, 30.0, 28.5, 27.2, 27.2, 27.0, 19.7; HRMS (ESI-TOF) *m*/*z*: $[M + Na]^+$ calcd for $C_{34}H_{44}NaO_6Si$ 599.2805, found 599.2783.

3-*O*-Benzyl-(*S*)-5-*O*-[(1,1-dimethylethyl) diphenylsilyl]-1,2-*O*-isopropylidene-5-*C*-*p*-toluenesulfonyloxypropyl-α-D-ribose (10). Under argon atmosphere, *p*-TsCl (5.98 g, 31.36 mmol) and pyridine (5.2 mL, 62.71 mmol) were added to a solution of compound **9** (5.17 g, 8.96 mmol) in CH_2Cl_2 (52 mL) at 0 °C. The mixture was stirred for 16 h at room temperature. The mixture was extracted with $CHCl_3$ and saturated $NaHCO_3$ aqueous solution; organic layer was washed with brine. The organic layer was dried over N_2SO_4, filtered, and concentrated. The crude

 © 2022 The Author(s). Published by the Royal Society of Chemistry

material was purified by column chromatography (17% ethyl acetate in hexane) to afford desired product **10** as a colorless oil (6.19 g, 8.47 mmol, 95%). ^{1}H NMR (600 MHz, $CDCl_3$): δ 7.67–7.65 (m, 6H), 7.42–7.39 (m, 2H), 7.34–7.26 (m, 11H), 5.71 (d, *J* = 3.0 Hz, 1H), 4.64 (d, *J* = 10.8 Hz, 1H), 4.52 (t, *J* = 4.2 Hz, 1H), 4.33 (d, *J* = 10.8 Hz, 1H), 4.00 (dd, *J* = 8.4, 2.4 Hz, 1H), 3.84–3.81 (m, 2H), 3.73–3.65 (m, 2H), 2.43 (s, 3H), 1.58–1.55 (m, 1H), 1.53 (s, 3H), 1.53–1.48 (m, 2H), 1.43–1.37 (m, 1H), 1.35 (s, 3H), 1.00 (s, 9H); ^{13}C {^{1}H}NMR (151 MHz, $CDCl_3$): δ 144.6, 137.7, 136.1, 136.0, 134.1, 133.8, 133.2, 129.9, 129.8, 129.8, 128.5, 128.2, 128.0, 128.0, 127.7, 113.0, 104.3, 80.8, 78.1, 77.8, 72.0, 71.9, 70.5, 29.8, 27.1, 26.9, 24.6, 21.7, 19.6; HRMS (ESI-TOF) *m*/*z*: [M + Na]$^+$ calcd for $C_{41}H_{50}NaO_8SSi$ 753.2893, found 753.2886.

(*S*)-5-*C*-azidopropyl-3-*O*-benzyl-5-*O*-[(1,1-dimethylethyl)diphenylsilyl]-1,2-*O*-isopropylidene-α-D-ribose (11). Under argon atmosphere, NaN_3 (4.63 g, 71.15 mmol) was added to a solution of compound **10** (6.19 g, 8.47 mmol) in DMF (62 mL). The mixture was stirred for 8 h at 60 °C. The mixture was extracted with ethyl acetate and brine. The organic layer was dried over Na_2SO_4, filtered, and concentrated. The crude material was purified by column chromatography (9% ethyl acetate in hexane) to afford desired product **11** as a colorless oil (4.57 g, 7.59 mmol, 81%) ^{1}H NMR (600 MHz, $CDCl_3$): δ 7.71–7.68 (m, 4H), 7.43–7.40 (m, 2H), 7.36–7.30 (m, 9H), 5.76 (d, *J* = 3.6 Hz, 1H), 4.68 (d, *J* = 10.8, 1H), 4.56 (t, *J* = 4.2 Hz, 1H), 4.37 (d, *J* = 10.8, 1H), 4.07 (dd, *J* = 8.1, 2.4 Hz, 1H), 3.92 (dd, *J* = 8.7, 4.2 Hz, 1H), 3.89–3.87 (m, 1H), 2.92–2.86 (m, 2H), 1.65–1.63 (m, 1H), 1.56 (s, 3H), 1.45–1.40 (m, 3H), 1.36 (s, 3H), 1.02 (s, 9H); ^{13}C {^{1}H}NMR (151 MHz, $CDCl_3$): δ 137.8, 136.1, 136.1, 134.3, 133.9, 129.8, 129.8, 128.5, 128.1, 128.0, 127.7, 127.7, 113.0, 104.4, 80.8, 78.2, 77.9, 72.1, 72.0, 51.3, 31.0, 27.2, 27.0, 24.7, 19.7; HRMS (ESI-TOF) *m*/*z*: [M + Na]$^+$ calcd for $C_{34}H_{43}N_3NaO_5Si$ 624.2870, found 624.2843.

(*S*)-5-*C*-Azidopropyl-3-*O*-benzyl-1,2-*O*-diacetyl-5-*O*-[(1,1-dimethylethyl)diphenylsilyl]-β-D-ribose (12). To a solution of **11** in CH_2Cl_2 (20 mL) was added 50% CF_3CO_2H aqueous solution (120 mL) and stirred for 4.5 h at room temperature. The mixture was washed with saturated $NaHCO_3$ aqueous and brine, dried (Na_2SO_4). After concentration, the residue was dissolved in pyridine (130 mL). Acetic anhydride (32.6 mL, 350.8 mmol) was added to the mixture under argon atmosphere. After the reaction mixture was stirred for 20 h at room temperature, the mixture was washed with saturated $NaHCO_3$ aqueous and brine, dried (Na_2SO_4). After concentration, the residue was purified by a silica gel column chromatography (hexane : EtOAc = 4 : 1) to afford desired product **12** as a colorless oil (11.89 g, 18.41 mmol, 81%). β-anomer: ^{1}H NMR (600 MHz, $CDCl_3$): δ 7.70–7.68 (m, 4H), 7.45–7.29 (m, 10H), 6.16 (s, 1H), 5.35 (d, *J* = 4.2 Hz, 1H), 4.57 (d, *J* = 10.8 Hz, 1H), 4.43 (dd, *J* = 8.4, 4.2 Hz, 1H), 4.33 (d, *J* = 10.8 Hz, 1H), 4.09 (dd, *J* = 8.4, 3.6 Hz, 1H), 3.86–3.84 (m, 1H), 2.89–2.75 (m, 2H), 2.13 (s, 3H), 1.97 (s, 3H), 1.67–1.60 (m, 1H), 1.47–1.40 (m, 1H), 1.36–1.25 (m, 2H), 1.06 (s, 9H); ^{13}C {^{1}H}NMR (151 MHz, $CDCl_3$) δ 170.0, 169.4, 137.3, 136.0, 136.0, 134.3, 133.5, 130.0, 129.9, 128.6, 128.2, 128.1, 127.8, 127.7, 98.2, 83.2, 76.7, 74.0, 73.4, 72.2, 51.3, 30.6, 27.1, 24.4, 21.3, 20.9, 19.7; HRMS (ESI-TOF) *m*/*z*: [M + Na]$^+$ calcd for $C_{35}H_{43}N_3NaO_7Si$ 688.2768, found 688.2769.

2′-*O*-Acetyl-(*S*)-5′-*C*-azidopropyl-6-*N*-benzoyl-3′-*O*-benzyl-5′-*O*-[(1,1-dimethylethyl)diphenylsilyl]adenosine (13). Under argon atmosphere, 1 M $SnCl_4$ in CH_2Cl_2 (14.69 mL, 14.69 mmol) was added to a solution of **12** (6.32 g, 9.79 mmol) and N^6-benzoyl adenine (2.81 g, 11.75 mmol) in CH_3CN (63 mL) at −20 °C. After the reaction mixture was stirred for 2 h at room temperature, the mixture was quenched with saturated $NaHCO_3$ aqueous. The mixture was extracted with saturated $NaHCO_3$ aqueous and brine, dried (Na_2SO_4). After concentration, the residue was purified by a silica gel column chromatography (hexane : EtOAc = 1 : 1) to afford desired product **13** as a white form (5.65 g, 6.85 mmol, 70%). ^{1}H NMR (600 MHz, $CDCl_3$): δ 9.07 (s, 1H), 8.77 (s, 1H), 8.22 (s, 1H), 8.04 (d, *J* = 7.2 Hz, 2H), 7.62–7.58 (m, 5H), 7.53 (t, *J* = 7.2 Hz, 2H), 7.41–7.25 (m, 11H), 6.15 (d, *J* = 4.8 Hz, 1H), 5.82 (t, *J* = 4.2 Hz, 1H), 4.63 (t, *J* = 5.4 Hz, 1H), 4.60 (d, *J* = 11.4 Hz, 1H), 4.38 (d, *J* = 11.4 Hz, 1H), 4.13 (dd, *J* = 6.3, 3.6 Hz, 1H), 3.82–3.79 (m, 1H), 2.94–2.83 (m, 2H), 2.12 (s, 3H), 1.75–1.70 (m, 1H), 1.44–1.28 (m, 3H), 1.05 (s, 9H); ^{13}C {^{1}H}NMR (151 MHz, $CDCl_3$): δ 170.0, 164.7, 153.0, 151.6, 149.7, 141.7, 137.2, 136.0, 135.9, 133.8, 133.5, 133.1, 132.9, 130.0, 129.9, 129.0, 128.7, 128.3, 128.3, 128.1, 128.0, 127.8, 127.7, 123.5, 86.6, 84.2, 76.5, 74.5, 73.6, 72.8, 51.2, 30.6, 27.2, 24.6, 20.8, 19.5; HRMS (ESI-TOF) *m*/*z*: [M + K]$^+$ calcd for $C_{45}H_{48}KN_8O_6Si$ 863.3103, found 863.3113.

(*S*)-5′-*C*-Azidopropyl-6-*N*-benzoyl-3′-*O*-benzyl-5′-*O*-[(1,1-dimethylethyl)diphenylsilyl]adenosine (14). K_2CO_3 (1.89 g, 13.70 mmol) was added to a solution of compound **13** (5.65 g, 6.85 mmol) in methanol (56 mL), and the mixture was stirred for 30 min at 0 °C. The mixture was extracted with ethyl acetate and water; the organic layer was washed with brine. The organic layer was dried over Na_2SO_4, filtered, and concentrated. The crude material was purified by column chromatography (50% ethyl acetate in hexane) to afford desired product **14** as a white solid (4.96 g, 6.33 mmol, 92%). ^{1}H NMR (400 MHz, $CDCl_3$): δ 8.97 (s, 1H), 8.76 (s, 1H), 8.15 (s, 1H), 8.05–8.03 (m, 2H), 7.66–7.53 (m, 7H), 7.44–7.28 (m, 11H), 5.98 (d, *J* = 5.2 Hz, 1H), 4.70 (dd, *J* = 11.4, 6.0 Hz, 1H), 4.65 (d, *J* = 11.2 Hz, 1H), 4.56 (d, *J* = 12.0 Hz, 1H), 4.36 (t, *J* = 4.8 Hz, 1H), 4.11 (t, *J* = 3.6 Hz, 1H), 3.77–3.73 (m, 1H), 3.45 (d, *J* = 6.0 Hz, 1H), 2.99–2.83 (m, 2H), 1.74–1.68 (m, 1H), 1.45–1.38 (m, 2H), 1.30–1.26 (m, 1H), 1.02 (s, 9H); ^{13}C {^{1}H}NMR (151 MHz, $CDCl_3$): δ 164.7, 152.8, 151.6, 149.7, 141.7, 136.9, 135.9, 135.9, 133.8, 133.5, 133.0, 132.9, 130.1, 130.0, 129.0, 128.9, 128.7, 128.5, 128.0, 127.8, 127.7, 123.4, 88.8, 84.3, 78.0, 74.3, 73.4, 73.1, 51.2, 30.5, 27.1, 24.6, 19.6; HRMS (ESI-TOF) *m*/*z*: [M + Na]$^+$ calcd for $C_{43}H_{46}N_8NaO_5Si$ 805.3258, found 805.3243.

(*S*)-5′-*C*-Azidopropyl-6-*N*-benzoyl-3′-*O*-benzyl-5′-*O*-[(1,1-dimethylethyl)diphenylsilyl]-2-*O*-methyladenosine (15). NaH (0.63 g, 15.66 mmol) was added to a solution of compound **14** (4.09 g, 5.22 mmol) in THF (41 mL) at 0 °C. Then, CH_3I (1.6 mL, 26.10 mmol) was added in dropwise and stirred 2.5 hours at 0 °C. Saturated $NaHCO_3$ aqueous solution was added, then the mixture was extracted with ethyl acetate and saturated $NaHCO_3$ aqueous solution. The organic layer was washed with brine, dried over Na_2SO_4, filtered, and concentrated. The crude material was purified by column chromatography (50% ethyl

acetate in hexane) to afford desired product **15** as a white solid (2.99 g, 3.75 mmol, 72%). ^{1}H NMR (600 MHz, $CDCl_3$): δ 9.11 (s, 1H), 8.79 (s, 1H), 8.33 (s, 1H),8.04–8.03 (m, 2H), 7.65–7.60 (m, 5H), 7.54–7.52 (m, 2H), 7.43–7.30 (m, 11H), 6.18 (d, J = 4.2 Hz, 1H), 4.61 (d, J = 11.4 Hz, 1H), 4.48 (d, J = 11.4 Hz, 1H), 4.42 (t, J = 4.8 Hz, 1H), 4.36 (t, J = 5.4 Hz, 1H), 4.20 (dd, J = 5.7, 2.4 Hz, 1H), 3.85–3.82 (m, 1H), 3.48 (s, 3H), 2.93–2.85 (m, 2H), 1.83–1.75 (m, 1H), 1.48–1.39 (m, 2H), 1.30–1.23 (m, 1H), 1.06 (s, 9H); ^{13}C {^{1}H}NMR (151 MHz, $CDCl_3$): δ 164.7, 152.9, 151.5, 149.6, 141.7, 137.4, 136.0, 135.9, 133.9, 133.5, 132.9, 130.1, 130.0, 129.0, 128.6, 128.3, 128.0, 127.9, 127.8, 123.6, 86.8, 83.7, 82.4, 76.2, 72.9, 72.7, 58.7, 51.2, 30.8, 27.3, 27.2, 24.6, 19.6; HRMS (ESI-TOF) m/z: [M + Na]$^+$ calcd for 819.3415, found 819.3417.

(*S*)-5′-*C*-Azidopropyl-6-*N*-benzoyl-3′-*O*-benzyl-2′-*O*-methyladenosine (16). *n*-Tetrabuthylammonium fluoride (TBAF, 1.35 mL of a 1 M solution in THF) was added to a solution of compound **15** (0.72 g, 0.90 mmol) in THF (7.2 mL) at room temperature under argon atmosphere. After being stirred at room temperature for 16 h, the mixture was concentrated. The residue was purified by column chromatography (50% ethyl acetate in hexane) to afford desired product **16** as a white solid (0.46 g, 0.83 mmol, 92%). ^{1}H NMR (600 MHz, $CDCl_3$): δ 9.19 (s, 1H), 8.74 (s, 1H), 8.04 (s, 1H), 8.02–8.00 (m, 2H), 7.61–7.59 (m, 1H), 7.51 (t, J = 7.8 Hz, 2H), 7.14–7.32 (m, 5H), 5.99 (d, J = 7.2 Hz, 1H), 5.78 (d, J = 12.0 Hz, 1H), 4.74 (d, J = 12.0 Hz, 1H), 4.71 (d, J = 11.4 Hz, 1H), 4.68 (dd, J = 7.8, 4.8 Hz, 1H), 4.32 (d, J = 4.8 Hz, 1H), 4.27 (s, 1H), 3.61–3.57 (m, 1H), 3.29 (s, 3H), 3.27–3.26 (m, 2H), 1.79–1.75 (m, 1H), 1,66–1.62 (m, 2H), 1.58–1.53 (m, 1H); ^{13}C {^{1}H} (151 MHz, $CDCl_3$): δ 164.7, 152.0, 150.5, 143.4, 137.4, 133.5, 133.1, 129.0, 128.8, 128.4, 128.3, 128.0, 124.9, 89.8, 87.7, 81.7, 77.6, 72.7, 72.1, 58.6, 51.4, 31.1, 25.5; HRMS (ESI-TOF) m/z: [M + Na]$^+$ calcd for $C_{28}H_{30}N_8NaO_5$ 581.2237, found 581.2238.

(*S*)-5′-*C*-Azidopropyl-6-*N*-benzoyl-2′-*O*-methyladenosine (17). Under argon atmosphere, BCl_3 (4.96 mL of a 1 M solution in CH_2Cl_2) was added to a solution of compound **16** (0.46 g, 0.83 mmol) in CH_2Cl_2 (6.9 mL) at −78 °C. After the mixture was stirred at −78 °C for 3 h, the reaction mixture was quenched with 50% Et_3N in EtOH. After concentration, the residue was purified by column chromatography (5% methanol in $CHCl_3$) to afford desired product **17** as a white solid (0.35 g, 0.74 mmol, 89%). ^{1}H NMR (400 MHz, $CDCl_3$): δ 9.04 (s, 1H), 8.80 (s, 1H), 8.07 (s, 1H), 8.04–8.02 (m, 2H), 7.66–7.62 (m, H), 7.55 (t, J = 7.6 Hz, 2H), 5.93 (d, J = 7.6 Hz, 1H), 5.78 (d, J = 12.0 Hz, 1H), 4.74 (dd, J = 7.2, 4.4 Hz, 1H), 4.58 (d, J = 4.4 Hz, 1H), 4.28 (s, 1H), 3.80–3.74 (m, 1H), 3.37 (s, 3H), 3.31 (t, J = 6.4 Hz, 2H), 2.72 (d, J = 1.2 Hz, 1H), 1.85–1.80 (m, 1H), 1.72–1.60 (m, 3H); ^{13}C {^{1}H}NMR (151 MHz, $CDCl_3$): δ 164.8, 152.2, 150.7, 150.6, 143.3, 133.5, 133.2, 129.1, 128.1, 124.8, 89.5, 89.4, 82.3, 71.9, 71.3, 59.0, 51.4, 31.0, 25.5; HRMS (ESI-TOF) m/z: [M + Na]$^+$ calcd for $C_{21}H_{24}N_8NaO_5$ 491.1767, found 491.1781.

(*S*)-5′-*C*-Azidopropyl-6-*N*-benzoyl-3′-*O*-[(1,1-dimethylethyl)diphenylsilyl]-2′-*O*-methyladenosine (18). Under argon atmosphere, imidazole (1.16 g, 17.08 mmol), TBDPSCl (1.48 mL, 5.69 mmol) was added to a solution of **17** (2.05 g, 4.38 mmol) in DMF (20 mL) at 0 °C, and the mixture was stirred for 24 h at 0 °C. The mixture was extracted with ethyl acetate and water. The organic layer was washed with brine, dried over Na_2SO_4, filtered, and concentrated. The crude material was purified by column chromatography (50% ethyl acetate in hexane) to afford desired product **18** as a white solid (2.36 g, 3.34 mmol, 76%). ^{1}H NMR (600 MHz, $CDCl_3$): δ 9.14 (s, 1H), 8.70 (s, 1H), 8.13 (s, 1H), 8.02 (d, J = 7.2 Hz, 2H), 7.75–7.70 (m, 4H), 7.62–7.60 (m, 1H), 7.53–7.40 (m, 8H), 6.06 (d, J = 6.6 Hz, 1H), 5.64 (d, J = 11.4 Hz, 1H), 4.56–4.54 (m, 2H), 4.00 (d, J = 1.2 Hz, 1H), 3.15 (s, 3H), 3.15–3.12 (m, 2H), 2.95–2.92 (m, 1H), 1.54–1.50 (m, 1H), 1.47–1.42 (m, 2H), 1.31–1.24 (m, 1H), 1.16 (s, 1H); ^{13}C {^{1}H}NMR (151 MHz, $CDCl_3$): δ 164.6, 152.0, 150.6, 150.5, 143.5, 136.1, 136.0, 133.6, 133.5, 133.1, 133.0, 130.3, 130.2, 129.0, 128.1, 128.0, 128.0, 124.9, 90.6, 89.7, 82.1, 73.0, 71.0, 58.9, 51.2, 30.9, 27.1, 25.3, 19.5; HRMS (ESI-TOF) m/z: [M + Na]$^+$ calcd for $C_{37}H_{42}N_8NaO_5Si$ 729.2945, found 729.2958.

(*S*)-5′-*C*-Azidopropyl-6-*N*-benzoyl-5′-*O*-(4,4′-dimethoxytrityl)-3′-*O*-[(1,1-dimethylethyl)diphenylsilyl]-2′-*O*-methyladenosine (19). Under argon atmosphere, DMTrCl (0.50 g, 1.46 mmol), $AgNO_3$ (0.25 g, 1.46 mmol) were added to a solution of **18** (0.52 g, 0.73 mmol) in THF/pyridine (v : v = 3 : 1, 16 mL) at room temperature, and the mixture was stirred for 12 h at 40 °C. The mixture was filtered through Celite, and the filtrate was extracted with ethyl acetate and water. The organic layer was washed with brine, dried over Na_2SO_4, filtered, and concentrated. The crude material was purified by column chromatography (33% ethyl acetate in hexane) to afford desired product **19** as a yellow solid (0.53 g, 0.53 mmol, 72%). ^{1}H NMR (600 MHz, $CDCl_3$): δ 9.05 (s, 1H), 8.80 (s, 1H), 8.40 (s, 1H), 8.06–8.05 (m, 2H), 7.63–7.60 (m, 3H), 7.55–7.49 (m, 4H), 7.44–7.37 (m, 4H), 7.33 (t, J = 7.8 Hz, 2H), 7.26–7.23 (m, 7H), 7.18–7.16 (m, 2H), 6.70–6.66 (m, 4H), 6.22 (d, J = 7.2 Hz, 1H), 4.86 (dd, J = 7.8, 4.8 Hz, 1H), 4.51 (dd, J = 4.8, 1.2 Hz, 1H), 3.96 (dd, J = 2.7, 1.2 Hz, 1H), 3.77 (s, 3H), 3.76 (s, 3H), 3.13 (s, 3H), 3.01–2.99 (m, 1H), 2.78–2.73 (m, 1H), 2.67–2.62 (m, 1H), 1.40–1.34 (m, 1H), 1.08 (s, 9H), 1.06–1.02 (m, 1H), 0.98–0.91 (m, 1H), 0.56–0.49 (m, 1H); ^{13}C {^{1}H}NMR (151 MHz, $CDCl_3$): δ 164.7, 158.7, 158.6, 152.9, 152.4, 149.6, 146.2, 142.7, 136.6, 136.2, 136.1, 135.8, 133.9, 133.8, 133.2, 132.9, 130.6, 130.5, 130.1, 129.9, 129.0, 128.4, 128.0, 127.9, 127.7, 126.9, 123.9, 113.1, 113.0, 87.2, 86.7, 85.7, 82.4, 74.1, 72.1, 58.6, 55.4, 51.1, 27.8, 27.1, 19.5; HRMS (ESI-TOF) m/z: [M + Na]$^+$ calcd for $C_{58}H_{60}N_8NaO_7Si$ 1031.4252, found 1031.4272.

6-*N*-Benzoyl-(*S*)-5′-*O*-(4,4′-dimethoxytrityl)-3′-*O*-[(1,1-dimethylethyl)diphenylsilyl]-2′-*O*-methyl-5′-*C*-trifluoroacetylaminopropyladenosine (20). Ph_3P (1.46 g, 5.55 mmol) and H_2O (1.6 mL, 88.8 mmol) were added to a solution of compound **19** (2.24 g, 2.22 mmol) in THF (44 mL). After being stirred at 40 °C for 12 h, the mixture was concentrated *in vacuo*. The residue was dissolved in CH_2Cl_2 (20 mL). Et_3N (0.46 mL, 3.33 mmol) and CF_3CO_2Et (0.79 mL, 6.66 mmol) were added to the mixture. After being stirred at room temperature for 24 h, the mixture was extracted with ethyl acetate and water. The organic layer was washed with brine, dried over Na_2SO_4, filtered, and concentrated. The crude material was purified by column chromatography (33% ethyl acetate in hexane) to afford desired product **20** as a yellow solid (2.22 g, 2.06 mmol, 93%). ^{1}H NMR (600 MHz, $CDCl_3$): δ 9.04 (s, 1H), 8.80 (s, 1H), 8.38 (s, 1H), 8.06

 © 2022 The Author(s). Published by the Royal Society of Chemistry

(d, J = 7.8 Hz, 2H), 7.63–7.58 (m, 3H), 7.54 (t, J = 7.8 Hz, 2H), 7.49 (d, J = 6.6 Hz, 2H), 7.45–7.42 (m, 1H), 7.39–7.37 (m, 2H), 7.36–7.32 (m, 3H), 7.26–7.23 (m, 6H), 7.17–7.16 (m, 3H), 6.69–6.65 (m, 4H), 6.20 (d, J = 7.2 Hz, 1H), 5.94 (bs, 1H), 4.92 (dd, J = 7.8, 4.8 Hz, 1H), 4.50 (dd, J = 4.8, 1.2 Hz, 1H), 3.92 (d, J = 1.2 Hz, 1H), 3.77 (s, 3H), 3.76 (s, 3H), 3.15 (s, 3H), 2.99–2.97 (m, 1H), 2.80–2.77 (m, 2H), 1.32–1.24 (m, 1H), 1.08 (s, 9H), 1.02–0.97 (m, 1H), 0.83–0.78 (m, 1H), 0.54–0.50 (m, 1H); ^{13}C {^{1}H}NMR (151 MHz, $CDCl_3$): δ 164.7, 158.7, 158.6, 152.9, 152.4, 149.7, 146.1, 142.2, 136.6, 136.1, 135.9, 134.0, 133.8, 133.0, 133.0, 130.5, 130.4, 130.0, 130.0, 129.1, 128.3, 128.0, 127.9, 127.8, 127.0, 123.9, 113.1, 113.0, 87.2, 86.6, 85.7, 82.1, 73.9, 72.1, 58.6, 55.4, 39.7, 27.6, 27.0, 19.5; HRMS (ESI-TOF) m/z: [M + Na]$^+$ calcd for $C_{60}H_{61}F_3N_6NaO_8Si$ 1101.4156, found 1101.4170.

6-*N*-Benzoyl-(*S*)-5′-*O*-(4,4′-dimethoxytrityl)-2′-*O*-methyl-5′-*C*-trifluoroacetylaminopropyladenosine (21). TBAF (1.31 mL of a 1 M solution in THF) was added to a solution of compound **20** (0.94 g, 0.87 mmol) in THF (9.4 mL) at room temperature under argon atmosphere. After being stirred at room temperature for 24 h, the mixture was concentrated. The residue was purified by column chromatography (66% ethyl acetate in hexane) to afford desired product **21** as a white solid (0.73 g, 0.87 mmol, 99%). ^{1}H NMR (600 MHz, $CDCl_3$): δ 9.09 (s, 1H), 8.77 (s, 1H), 8.20 (s, 1H), 8.04 (d, J = 7.2 Hz, 2H), 7.61 (t, J = 7.2 Hz, 1H), 7.53 (t, J = 7.8 Hz, 2H), 7.47 (d, J = 6.6 Hz, 2H), 7.36 (dd, J = 9.0, 3.0 Hz, 4H), 7.22 (t, J = 7.2 Hz, 2H), 7.19–7.16 (m, 1H), 6.78–6.74 (m, 4H), 6.43 (bs, 1H), 6.07 (d, J = 4.2 Hz, 1H), 4.61 (dd, J = 5.7, 4.2 Hz, 1H), 4.38 (d, J = 4.8 Hz, 1H), 4.12 (t, J = 4.8 Hz, 1H), 3.77 (s, 3H), 3.76 (s, 3H), 3.55 (dd, J = 11.1, 4.8 Hz, 1H), 3.53 (s, 3H), 3.90–2.97 (m, 2H), 2.84 (d, J = 4.8 Hz, 1H), 1.45–1.41 (m, 1H), 1.36–1.34 (m, 2H), 1.29–1.25 (m, 1H); ^{13}C {^{1}H}NMR (151 MHz, $CDCl_3$): δ 164.8, 158.8, 158.7, 157.6, 157.3, 157.1, 156.8, 152.8, 151.6, 149.8, 146.1, 142.0, 136.6, 136.5, 133.7, 133.0, 130.1, 129.1, 128.5, 128.0, 127.8, 127.1, 123.9, 118.8, 116.8, 114.9, 113.2, 113.1, 113.0, 87.1, 87.0, 86.7, 85.5, 82.7, 73.5, 69.8, 59.1, 55.3, 40.0, 28.1, 24.2; HRMS (ESI-TOF) m/z: [M + Na]$^+$ calcd for $C_{44}H_{43}F_3N_6NaO_8$ 863.2992, found 863.2966.

6-*N*-Benzoyl-3′-*O*-[2-cyanoethoxy(diisopropylamino) phosphino]-(*S*)-5′-*O*-(4,4′-dimethoxytrityl)-2′-*O*-methyl-5′-*C*-trifluoroacetylaminopropyladenosine (22). Under argon atmosphere, DIPEA (1.31 mL, 7.5 mmol), 2-cyanoethyl-*N*,*N*-diisopropylchlorophosphoroamidite (0.67 mL, 3.0 mmol) were added to a solution of **21** (1.26 g, 1.50 mmol) in THF (13 mL) at room temperature, and the mixture was stirred for 1 h. The mixture was extracted with ethyl acetate and saturated $NaHCO_3$ aqueous solution. The organic layer was washed with brine, dried over Na_2SO_4, filtered, and concentrated. The crude material was purified by column chromatography (50% ethyl acetate in hexane) to afford desired product **22** as a white solid (1.25 g, 1.20 mmol, 80%) ^{31}P NMR (151 MHz, $CDCl_3$): δ 151.7, 150.2; HRMS (ESI-TOF) m/z: [M + K]$^+$ calcd for $C_{53}H_{60}F_3KN_8O_9P$ 1079.3810, found 1079.3836.

2′-*O*-Acetyl-(*S*)-5′-*C*-azidopropyl-3′-*O*-benzyl-6-chloro-5′-*O*-[(1,1-dimethylethyl)diphenylsilyl] guanosine (23). *N*,*O*-Bis(-trimethylsilyl)acetamide (2.0 mL, 8.16 mmol) was added to a solution of **12** (1.75 g, 2.72 mmol) and 2-amino-6-chloropurine (0.51 g, 2.99 mmol) in toluene (15 mL). The mixture was stirred for 1 h at 80 °C. The solution was cooled to 0 °C, and TMSOTf (1.0 mL, 5.44 mmol) was added in dropwise; the mixture was warmed to 80 °C and stirred for 15 h. The mixture was extracted with ethyl acetate and saturated $NaHCO_3$ aqueous solution. The organic layer was washed with brine, dried over Na_2SO_4, filtered, and concentrated. The crude material was purified by column chromatography (33% ethyl acetate in hexane) to afford desired product **23** as a white solid (1.54 g, 2.04 mmol, 75%). ^{1}H NMR (600 MHz, $CDCl_3$): δ 7.96 (s, 1H), 7.63–7.59 (m, 4H), 7.42–7.29 (m, 10H), 7.26–7.25 (m, 1H), 5.97 (d, J = 4.8 Hz, 1H), 5.73 (t, J = 4.8 Hz, 1H), 5.14 (s, 2H), 4.59 (d, J = 10.8 Hz, 1H), 4.53 (t, J = 5.4 Hz, 1H), 4.37 (d, J = 11.4 Hz, 1H), 4.10 (dd, J = 5.4, 3.6 Hz, 1H), 3.78–3.75 (m, 1H), 2.95–2.91 (m, 1H), 2.86–2.81 (m, 1H), 2.12 (s, 3H), 1,72–1.69 (m, 1H), 1.41–1.38 (m, 2H), 1.30–1.26 (m, 1H), 1.05 (s, 9H); ^{13}C {^{1}H}NMR (151 MHz, $CDCl_3$): δ 170.0, 159.1, 153.4, 151.7, 140.8, 137.2, 136.0, 135.9, 133.5, 133.1, 130.1, 129.9, 128.7, 128.4, 128.3, 127.8, 127.7, 125.9, 86.0, 84.3, 76.4, 74.2, 73.5, 72.8, 51.1, 30.4, 27.2, 24.6, 20.8, 19.6; HRMS (ESI-TOF) m/z: [M + Na]$^+$ calcd for $C_{38}H_{43}ClN_8NaO_5Si$ 777.2712, found 777.2700.

(*S*)-5′-*C*-Azidopropyl-3′-*O*-benzyl-6-chloro-5′-*O*-[(1,1-dimethylethyl)diphenylsilyl] guanosine (24). K_2CO_3 (2.77 g, 20.18 mmol) was added to a solution of **23** (8.00 g, 10.59 mmol) in methanol (80 mL), and the mixture was stirred for 30 min at 0 °C. The mixture was extracted with ethyl acetate and water; the organic layer was washed with brine. The organic layer was dried over Na_2SO_4, filtered, and concentrated. The crude material was purified by column chromatography (33% ethyl acetate in hexane) to afford desired product **24** as a white solid (7.03 g, 9.86 mmol, 93%). ^{1}H NMR (600 MHz, $CDCl_3$): δ 7.95 (s, 1H), 7.61–7.59 (m, 4H), 7.44–7.28 (m, 11H), 5.80 (d, J = 5.4 Hz, 1H), 5.03 (s, 2H), 4.64–4.60 (m, 2H), 4.54 (d, J = 11.4 Hz, 1H), 4.28 (dd, J = 5.4, 4.2 Hz, 1H), 4.07 (t, J = 4.2 Hz, 1H), 3.74–3.71 (m, 1H), 3.22 (d, J = 7.2 Hz, 1H), 2.98–2.94 (m, 1H), 2.86–2.82 (m, 1H), 1.75–1.70 (m, 1H), 1.42–1.34 (m, 2H), 1.28–1.24 (m, 1H), 1.04 (s, 9H); ^{13}C {^{1}H}NMR (151 MHz, $CDCl_3$): δ 159.1, 153.5, 151.6, 140.7, 136.7, 135.9, 135.9, 133.5, 132.8, 130.2, 130.1, 128.9, 128.7, 128.4, 127.9, 127.8, 125.8, 88.2, 84.1, 77.8, 74.1, 73.4, 73.1, 51.1, 30.4, 27.3, 24.6, 19.6; HRMS (ESI-TOF) m/z: [M + Na]$^+$ calcd for $C_{36}H_{41}ClN_8NaO_4Si$ 735.2606, found 735.2599.

(*S*)-5′-*C*-Azidopropyl-3′-*O*-benzyl-6-chloro-5′-*O*-[(1,1-dimethylethyl)diphenylsilyl]-2′-*O*-methyl-guanosine (25). CH_3I (1.84 mL, 29.58 mmol) and NaH (0.43 g, 10.85 mmol) were added to a solution of **24** (7.03 g, 9.86 mmol) and molecular sieve 3 Å (7.0 g) in DMF (70 mL) at 0 °C under argon atmosphere. After this solution was stirred 7 hours at 0 °C, the reaction was quenched with saturated $NaHCO_3$ aqueous solution. The mixture was extracted with ethyl acetate and saturated $NaHCO_3$ aqueous solution. The organic layer was washed with brine, dried over Na_2SO_4, filtered, and concentrated. The crude material was purified by column chromatography (33% ethyl acetate in hexane) to afford desired product **25** as a white solid (4.95 g, 6.81 mmol, 69%). ^{1}H NMR (600 MHz, $CDCl_3$): δ 8.08 (s, 1H), 7.64–7.61 (m, 4H), 7.37–7.31 (m, 11H), 6.00 (d, J = 3.6 Hz, 1H), 5.11 (s, 2H), 4.64 (d, J = 12.0 Hz, 1H), 4.48 (d, J = 11.4 Hz, 1H), 4.28 (d, J = 4.2 Hz, 1H), 4.15–4.13 (m, 1H), 3.79–3.76 (m, 1H), 3.43 (s, 3H), 2.95–2.90 (m, 1H), 2.85–2.80 (m, 1H), 1.80–1.74 (m,

© 2022 The Author(s). Published by the Royal Society of Chemistry

1H), 1.42–1.35 (m, 2H), 1.28–1.20 (m, 1H), 1.06 (s, 9H); ^{13}C {^{1}H} NMR (151 MHz, $CDCl_3$): δ 159.1, 153.5, 151.6, 140.6, 137.5, 136.0, 135.9, 133.5, 132.8, 130.2, 130.1, 128.7, 128.3, 127.9, 127.8, 125.9, 86.0, 83.8, 82.6, 76.2, 72.9, 72.9, 58.7, 51.2, 30.6, 27.3, 24.6, 19.7; HRMS (ESI-TOF) *m/z*: $[M + Na]^+$ calcd for $C_{37}H_{43}ClN_8NaO_4Si$ 749.2763, found 749.2741.

(*S*)-5′-*C*-Azidopropyl-3′-*O*-benzyl-5′-*O*-[(1,1-dimethylethyl) diphenylsilyl]-2′-*O*-methyl-guanosine (26). NaH (0.40 g, 10.00 mmol) was added to a solution of 3-hydroxypropionitrile (0.68 mL, 10.00 mmol) in THF (25 mL) at 0 °C under argon atmosphere. After this solution was stirred 10 min at 0 °C, compound **25** (3.64 g, 5.00 mmol) in THF (25 mL) was added to the reaction mixture at 0 °C; the mixture was stirred for 6 h at 0 °C. The reaction was quenched with saturated NH_4Cl aqueous solution and extracted with ethyl acetate and water. The organic layer was washed with brine, dried over Na_2SO_4, filtered, and concentrated. The crude material was purified by column chromatography (5% methanol in $CHCl_3$) to afford desired product **26** as a white solid (3.02 g, 4.26 mmol, 85%). ^{1}H NMR (600 MHz, $CDCl_3$): δ 12.09 (s, 1H), 7.88 (s, 1H), 7.69–7.62 (m, 4H), 7.44–7.40 (m, 2H), 7.37–7.29 (m, 9H), 6.10 (s, 2H), 5.97 (d, *J* = 4.2 Hz, 1H), 4.60 (d, *J* = 11.4 Hz, 1H), 4.44 (d, *J* = 12.0 Hz, 1H), 4.30 (t, *J* = 5.4 Hz, 1H), 4.17–4.14 (m, 2H), 3.84–3.81 (m, 1H), 3.47 (s, 3H), 2.94–2.90 (m, 1H), 2.87–2.81 (m, 1H), 1.83–1.77 (m, 1H), 1.43–1.39 (m, 2H), 1.28–1.22 (m, 1H), 1.07 (s, 9H); ^{13}C {^{1}H} NMR (151 MHz, $CDCl_3$): δ 159.3, 153.9, 151.4, 137.5, 136.0, 136.0, 135.5, 133.6, 132.9, 130.2, 130.1, 128.6, 128.3, 128.2, 127.9, 127.9, 117.7, 86.1, 83.2, 82.7, 76.1, 72.7, 58.6, 51.2, 30.8, 27.3, 24.6, 19.7; HRMS (ESI-TOF) *m/z*: $[M + Na]^+$ calcd for $C_{37}H_{44}N_8NaO_5Si$ 731.3102, found 731.3082.

(*S*)-5′-*C*-Azidopropyl-3′-*O*-benzyl-5′-*O*-[(1,1-dimethylethyl) diphenylsilyl]-2-*N*-isobutyryl-2′-*O*-methyl-guanosine (27). Isobutylic anhydride (2.84 g, 17.04 mmol) was added to a solution of **26** (3.02 g, 4.26 mmol) and DMAP (0.21 g, 1.70 mmol) in DMF (25 mL) at room temperature under argon atmosphere; the mixture was warmed to 60 °C and stirred for 13 h. The reaction was quenched with methanol and extracted with ethyl acetate and saturated $NaHCO_3$ aqueous solution. The organic layer was washed with brine, dried over Na_2SO_4, filtered, and concentrated. The crude material was purified by column chromatography (33% ethyl acetate in hexane) to afford desired product **27** as a white solid (2.57 g, 3.30 mmol, 77%). ^{1}H NMR (600 MHz, $CDCl_3$): δ 12.08 (s, 1H), 8.61 (s, 1H), 8.03 (s, 1H), 7.66–7.62 (m, 4H), 7,46–7,42 (m, 2H), 7.38–7.28 (m, 9H), 5.96 (d, *J* = 5.4 Hz, 1H), 4.61 (d, *J* = 11.4 Hz, 1H), 4.46 (d, *J* = 11.4 Hz, 1H), 4.25 (t, *J* = 4.8 Hz, 1H), 4.15 (t, *J* = 4.8 Hz, 1H), 4.12 (dd, *J* = 4.8, 2.4 Hz, 1H), 3.78–3.75 (m, 1H), 3.37 (s, 3H), 2.92–2.88 (m, 1H), 2.82–2.78 (m, 1H), 2.63–2.56 (m, 1H), 1.81–1.73 (m, 1H), 1.41–1.32 (m, 2H), 1.24 (d, *J* = 7.2 Hz, 6H), 1.20–1.16 (m, 1H), 1.06 (s, 9H); ^{13}C {^{1}H}NMR (151 MHz, $CDCl_3$): δ 178.6, 155.7, 148.2, 17.6, 137.4, 137.0, 136.0, 135.9, 133.4, 132.7, 130.3, 130.1, 128.7, 128.3, 128.0, 127.9, 121.8, 85.7, 83.9, 83.3, 76.1, 72.9, 72.8, 58.7, 51.1, 36.6, 30.6, 27.3, 24.6, 19.6, 19.1, 19.1; HRMS (ESI-TOF) *m/z*: $[M + Na]^+$ calcd for $C_{41}H_{50}N_8NaO_6Si$ 801.3520, found 801.3532.

(*S*)-5′-*C*-Azidopropyl-3′-*O*-benzyl-2-*N*-isobutyryl-2′-*O*-methyl-guanosine (28). *n*-Tetrabuthylammonium fluoride (TBAF, 2.56 mL of a 1 M solution in THF) was added to a solution of compound **27** (1.31 g, 1.71 mmol) in THF (13 mL) at room temperature under argon atmosphere. After being stirred at room temperature for 46 hours, the mixture was concentrated. The residue was purified by column chromatography (66% ethyl acetate in hexane) to afford desired product **28** as a white solid (0.77 g, 1.42 mmol, 83%). ^{1}H NMR (600 MHz, $CDCl_3$): δ 12.03 (s, 1H), 8.21 (s, 1H), 7.73 (s, 1H), 7.39–7.33 (m, 5H), 5.86 (d, *J* = 6.6 Hz, 1H), 5.21 (d, *J* = 10.8 Hz, 1H), 4.75 (d, *J* = 12.6 Hz, 1H), 4.67 (d, *J* = 11.4 Hz, 1H), 4.35 (dd, *J* = 7.5, 4.8 Hz, 1H), 4.22 (dd, *J* = 5.1, 1.2 Hz, 1H), 4.19 (s, 1H), 3.62–3.57 (m, 1H), 3.34–3.27 (m, 5H), 2.66–2.62 (m, 1H), 1.74–1.63 (m, 3H), 1.58–1.54 (m, 1H), 1.28 (dd, *J* = 6.9, 3.0 Hz, 6H); ^{13}C {^{1}H}NMR (151 MHz, $CDCl_3$): δ 178.7, 155.3, 147.6, 147.0, 139.1, 137.4, 128.7, 128.4, 128.3, 122.7, 88.7, 86.7, 82.3, 72.8, 71.8, 58.6, 51.2, 36.6, 31.4, 25.5, 19.0, 19.0; HRMS (ESI-TOF) *m/z*: $[M + Na]^+$ calcd for $C_{25}H_{32}N_8NaO_6$ 563.2343, found 563.2340.

(*S*)-5′-*C*-Azidopropyl-3′-*O*-[(1,1-dimethylethyl)diphenylsilyl]-2-*N*-isobutyryl-2′-*O*-methyl-guanosine (29). Under argon atmosphere, BCl_3 (8.30 mL of a 1 M solution in CH_2Cl_2) was added to a solution of compound **28** (0.75 g, 1.38 mmol) in CH_2Cl_2 (11 mL) at −78 °C. After the mixture was stirred at −78 °C for 4 h, the mixture was warmed to −50 °C and stirred for 4 hours. The reaction mixture was quenched with 7 M solution of aqueous NH_3 in methanol. After concentration, the residue was purified by column chromatography (10% methanol in $CHCl_3$) to afford a white solid compound. This compound was in DMF (5 mL), and imidazole (0.27 g, 4.02 mmol), TBDPSCl (0.35 mL, 1.34 mmol) was added at 0 °C under argon atmosphere and the mixture was stirred for 29 hours. The mixture was extracted with ethyl acetate and saturated $NaHCO_3$ aqueous solution. The organic layer was washed with brine, dried over Na_2SO_4, filtered, and concentrated. The crude material was purified by column chromatography (66% ethyl acetate in hexane) to afford desired product **29** as a white solid (0.48 g, 0.69 mmol, 50% in 2 steps). ^{1}H NMR (600 MHz, $CDCl_3$): δ 11.97 (s, 1H), 7.98 (s, 1H), 7.76 (s, 1H), 7.74–7.69 (m, 4H), 7.50–7.40 (m, 6H), 5.90 (d, *J* = 7.2 Hz, 1H), 5.18 (d, *J* = 10.2 Hz, 1H), 4.43 (d, *J* = 5.4 Hz, 1H), 4.18 (dd, *J* = 8.4, 4.8 Hz, 1H), 3.94 (s, 1H), 3.20–3.16 (m, 5H), 2.93–2.88 (m, 1H), 2.61–2.55 (m, 1H), 1.51–1.40 (m, 4H), 1.25 (dd, *J* = 7.5, 4.2 Hz, 6H), 1.14 (s, 9H); ^{13}C {^{1}H}NMR (151 MHz, $CDCl_3$): δ 178.4, 155.1, 147.5, 146.7, 139.3, 136.1, 136.0, 133.6, 133.0, 130.3, 130.2, 128.1, 127.9, 123.1, 89.7, 88.9, 82.5, 72.9, 71.2, 58.9, 51.1, 36.6, 31.3, 27.1, 25.3, 19.5, 19.0, 18.9; HRMS (ESI-TOF) *m/z*: $[M + Na]^+$ calcd for $C_{34}H_{44}N_8NaO_6Si$ 711.3051, found 711.3072.

(*S*)-5′-*C*-Azidopropyl-5′-*O*-(4,4′-dimethoxytrityl)-3′-*O*-[(1,1-dimethylethyl) diphenylsilyl]-2-*N*-isobutyryl-2′-*O*-methyl-guanosine (30). Under argon atmosphere, DMTrCl (0.89 g, 2.62 mmol), $AgNO_3$ (0.45 g, 2.62 mmol) were added to a solution of **29** (0.90 g, 1.31 mmol) in THF/pyridine (v : v = 3 : 1, 30 mL) at room temperature, and the mixture was stirred for 12 h at 40 °C. The mixture was filtered through Celite, and the filtrate was extracted with ethyl acetate and water. The organic layer was washed with brine, dried over Na_2SO_4, filtered, and concentrated. The crude material was purified by column chromatography (50% ethyl acetate in hexane) to afford desired product **30** as a yellow solid (1.19 g, 1.20 mmol, 92%). ^{1}H NMR (600 MHz, $CDCl_3$): δ 11.92 (s, 1H), 7.89 (s, 1H), 7.60–7.58 (m, 2H), 7.52–7.50

 © 2022 The Author(s). Published by the Royal Society of Chemistry

(m, 2H), 7.47–7.46 (m, 2H), 7.41–7.27 (m, 9H), 7.23–7.18 (m, 5H), 6.69 (dd, *J* = 10.8, 9.0 Hz, 4H), 5.83 (d, *J* = 7.8 Hz, 1H), 5.24 (dd, *J* = 7.8, 4.8 Hz, 1H), 4.59 (d, *J* = 5.4 Hz, 1H), 3.90 (s, 1H), 3.78 (s, 3H), 3.75 (s, 3H), 3.22 (s, 3H), 2.81–2.77 (m, 1H), 2.74 (dt, *J* = 9.0, 2.4 Hz, 1H), 2.66–2.62 (m, 1H), 1.50–1.45 (m, 1H), 1.24–1.20 (m, 1H), 1.08 (s, 9H), 0.91–0.85 (m, 1H), 0.66 (d, *J* = 6.6 Hz, 3H), 0.55 (d, *J* = 7.2 Hz, 3H), 0.44–0.36 (m, 1H); ^{13}C {^{1}H}NMR (151 MHz, $CDCl_3$): δ 178.0, 158.8, 158.8, 155.6, 148.4, 147.1, 146.9, 140.3, 136.7, 136.0, 135.8, 133.9, 133.0, 130.2, 130.0, 130.0, 129.9, 127.9, 127.9, 127.8, 127.7, 127.1, 123.2, 113.2, 86.7, 86.4, 86.3, 80.5, 74.7, 71.6, 58.8, 55.4, 55.3, 507, 36.1, 27.0, 24.8, 19.4, 18.5, 17.9, 17.8; HRMS (ESI-TOF) *m*/*z*: $[M + Na]^+$ calcd for $C_{55}H_{62}N_8NaO_8Si$ 1013.4363, found 1013.4358.

(*S*)-5′-*O*-(4,4′-dimethoxytrityl)-3′-*O*-[(1,1-dimethylethyl) diphenylsilyl]-2-*N*-isobutyryl-2′-*O*-methyl-5′-*C*-trifluoroacetylaminopropyl-guanosine (31). Ph_3P (0.79 g, 3.00 mmol) and H_2O (0.87 mL, 48.00 mmol) were added to a solution of compound **30** (1.19 g, 1.20 mmol) in THF (24 mL). After being stirred at 40 °C for 22 h, the mixture was concentrated *in vacuo*. The residue was dissolved in CH_2Cl_2 (10 mL). Et_3N (0.25 mL, 1.80 mmol) and CF_3CO_2Et (0.45 mL, 3.60 mmol) were added to the mixture. After being stirred at room temperature for 19 h, the mixture was extracted with ethyl acetate and water. The organic layer was washed with brine, dried over Na_2SO_4, filtered, and concentrated. The crude material was purified by column chromatography (50% ethyl acetate in hexane) to afford desired product **31** as a yellow solid (0.98 g, 0.92 mmol, 77% in 2 steps). ^{1}H NMR (600 MHz, $CDCl_3$): δ 11.93 (s, 1H), 7.85 (s, 1H), 7.59–7.57 (m, 2H), 7.51–7.49 (m, 2H), 7.47–7.45 (m, 2H), 7.41–7.27 (m, 9H), 7.21–7.17 (m, 5H), 6.69 (dd, *J* = 10.8, 9.0 Hz, 4H), 6.37 (t, *J* = 5.4 Hz, 1H), 5.81 (d, *J* = 9.0 Hz, 1H), 5.25 (dd, *J* = 8.1, 5.4 Hz, 1H), 4.61 (d, *J* = 5.4 Hz, 1H), 3.89 (s, 1H), 3.78 (s, 3H), 3.76 (s, 3H), 3.24 (s, 3H), 2.86–2.80 (m, 2H), 2.72–2.70 (m, 1H), 1.45–1.38 (m, 1H), 1.27–1.21 (m, 1H), 1.07 (s, 9H), 1.05–1.00 (m, 1H), 0.80–0.72 (m, 1H), 0.66 (d, *J* = 7.2 Hz, 3H), 0.54 (d, *J* = 6.6 Hz, 3H), 0.47–0.40 (m, 1H); ^{13}C {^{1}H}NMR (151 MHz, $CDCl_3$): δ 178.2, 158.9, 158.9, 155.6, 148.4, 147.1, 147.0, 140.3, 136.6, 136.1, 135.8, 134.0, 133.0, 130.1, 130.0, 130.0, 129.9, 128.0, 127.9, 127.8, 127.7, 127.2, 123.2, 113.3, 86.8, 86.4, 80.4, 74.6, 71.6, 58.8, 55.4, 55.4, 39.6, 36.1, 27.1, 24.5, 19.5, 18.6, 18.0, 17.9; HRMS (ESI-TOF) *m*/*z*: $[M + Na]^+$ calcd for $C_{57}H_{63}F_3N_6NaO_9Si$ 1083.4277, found 1083.4249.

(*S*)-5′-*O*-(4,4′-dimethoxytrityl)-2-*N*-isobutyryl-2′-*O*-methyl-5′-*C*-trifluoroacetylaminopropyl-guanosine (32). *n*-Tetrabuthylammonium fluoride (TBAF, 1.39 mL of a 1 M solution in THF) was added to a solution of compound **32** (0.98 g, 0.92 mmol) in THF (10 mL) at room temperature under argon atmosphere. After being stirred at room temperature for 19 hours, the mixture was concentrated. The residue was purified by column chromatography (100% ethyl acetate) to afford desired product **33** as a white solid (0.46 g, 0.56 mmol, 61%). ^{1}H NMR (600 MHz, $CDCl_3$): δ 12.11 (s, 1H), 8.43 (s, 1H), 7.72 (s, 1H), 7.54 (d, *J* = 6.6 Hz, 2H), 7.39 (d, *J* = 9.0 Hz, 4H), 7.25–7.18 (m, 3H), 6.79–6.76 (m, 4H), 6.37 (t, *J* = 5.4 Hz, 1H), 5.61 (d, *J* = 6.0 Hz, 1H), 4.90 (t, *J* = 6.0 Hz, 1H), 4.41–4.39 (m, 1H), 4.03 (t, *J* = 4.2 Hz, 1H), 3.77 (s, 3H), 3.77 (s, 3H), 3.44 (s, 3H), 3.36–3.33 (m, 1H), 3.12–3.06 (m, 1H), 2.98–2.93 (m, 1H), 2.70 (d, *J* = 3.6 Hz, 1H), 1.88–1.83 (m, 1H), 1.57–1.54 (m, 1H), 1.37–1.31 (m, 2H), 1.19–1.15 (m, 1H), 0.93 (d, *J* = 7.2 Hz, 3H), 0.84 (d, *J* = 7.2 Hz, 3H); ^{13}C {^{1}H}NMR (151 MHz, DMSO-d_6): δ 180.7, 158.6, 158.6, 156.6, 156.4, 155.3, 149.5, 148.8, 146.8, 137.8, 137.0, 136.8, 130.8, 130.7, 128.5, 128.1, 127.1, 121.0, 113.4, 113.4, 86.5, 86.2, 84.2, 82.3, 79.7, 73.5, 68.6, 58.2, 55.5, 55.5, 35.3, 28.2, 24.6, 19.4, 19.3; HRMS (ESI-TOF) *m*/*z*: $[M + Na]^+$ calcd for $C_{41}H_{45}F_3N_6NaO_9$ 845.3098, found 845.3108.

3′-*O*-[2-Cyanoethoxy(diisopropylamino)phosphino]-(*S*)-5′-*O*-(4,4′-dimethoxytrityl)-2-*N*-isobutyryl-2′-*O*-methyl-5′-*C*-trifluoroacetylaminopropylguanosine (33). Under argon atmosphere, DIPEA (0.50 mL, 2.81 mmol), 2-cyanoethyl-*N*,*N*-diisopropylchlorophosphoroamidite (0.25 mL, 1.12 mmol) were added to a solution of **33** (0.46 g, 0.56 mmol) in THF (4.6 mL) at room temperature, and the mixture was stirred for 1.5 h. The mixture was extracted with ethyl acetate and saturated $NaHCO_3$ aqueous solution. The organic layer was washed with brine, dried over Na_2SO_4, filtered, and concentrated. The crude material was purified by column chromatography (66% ethyl acetate in hexane) to afford desired product **34** as a white solid (0.38 g, 0.37 mmol, 65%). ^{31}P NMR (162 MHz, $CDCl_3$): δ 152.4, 150.8; HRMS (ESI-TOF) *m*/*z*: $[M + H]^+$ calcd for $C_{50}H_{63}F_3N_8O_{10}P$ 1023.4357, found 1023.4334.

(*S*)-5-*C*-Allyl-1,2-*O*-isopropylidene-3,5-*O*-(1,1,3,3-tetraisopropyl-1,3-disiloxandiyl)-α-D-ribose (34). To a solution of **6** in THF (2.0 mL) was added *n*-tetrabuthylammonium fluoride (TBAF, 0.52 mL of a 1 M solution in THF) under argon atmosphere. After being stirred at room temperature for 3.5 h, the mixture was concentrated. After concentration, the residue was purified by a silica gel column chromatography ($CHCl_3 : CH_3OH$ = 20 : 1). After the purified material was dissolved in pyridine (5.0 mL). 1,3-Dichloro-1,1,3,3-tetraisopropyldisiloxane ($TIPDSCl_2$, 0.16 mL, 0.50 mmol) was added to the reaction mixture in an ice bath under argon atmosphere. After being stirred at room temperature for 21 h, the mixture was extracted with ethyl acetate and saturated $NaHCO_3$ aqueous solution; the organic layer was washed with brine. The organic layer was dried over Na_2SO_4, filtered, and concentrated. The crude material was purified by column chromatography (2–5% ethyl acetate in hexane) to afford desired product **34** as a colorless oil (0.13 g, 0.28 mmol, 81% in 2 steps). ^{1}H NMR (400 MHz, $CDCl_3$): δ 5.87–5.77 (m, 1H), 5.72 (d, *J* = 3.6 Hz, 1H), 5.16 (dd, *J* = 17.0 Hz, 2.0 Hz, 1H), 5.07 (dd, *J* = 10.2 Hz, 2.0 Hz, 1H), 4.55 (t, *J* = 3.6 Hz, 1H), 4.06 (dd, *J* = 9.2 Hz, 3.6 Hz, 1H), 3.97–3.93 (m, 1H), 3.88 (dd, *J* = 9.0 Hz, 2.0 Hz, 1H), 2.57–2.41 (m, 2H), 1.56 (s, 3H), 1.36 (s, 3H), 1.11–1.04 (m, 28H); ^{13}C {^{1}H}NMR (151 MHz, $CDCl_3$): δ 134.4, 117.8, 113.1, 103.1, 79.4, 78.6, 71.5, 68.2, 38.4, 26.7, 26.6, 17.6, 17.5, 17.5, 17.4, 17.3, 17.2, 17.0, 13.7, 13.3, 13.3, 12.8, 12.7; HRMS (ESI-TOF) *m*/*z*: $[M + Na]^+$ calcd for $C_{23}H_{44}NaO_6Si_2$ 495.2574, found 495.2564.

(*R*)-5-*C*-Allyl-1,2-*O*-isopropylidene-3,5-*O*-(1,1,3,3-tetraisopropyl-1,3-disiloxandiyl)-α-D-ribose (35). To a solution of **7** in THF (2.5 mL) was added TBAF (0.77 mL of a 1 M solution in THF) under argon atmosphere. After being stirred at room temperature for 1 h, the mixture was concentrated. After concentration, the residue was purified by a silica gel column chromatography ($CHCl_3 : CH_3OH$ = 20 : 1). After the purified

© 2022 The Author(s). Published by the Royal Society of Chemistry

material was dissolved in pyridine (10 mL). 1,3-Dichloro-1,1,3,3-tetraisopropyldisiloxane ($TIPDSCl_2$, 0.32 mL, 1.02 mmol) was added to the reaction mixture in an ice bath under argon atmosphere. After being stirred at room temperature for 21 h, the mixture was extracted with ethyl acetate and saturated $NaHCO_3$ aqueous solution; the organic layer was washed with brine. The organic layer was dried over Na_2SO_4, filtered, and concentrated. The crude material was purified by column chromatography (2% ethyl acetate in hexane) to afford desired product **35** as a colorless oil (0.19 mg, 0.40 mmol, 79% in 2 steps). ^1H NMR (400 MHz, $CDCl_3$): δ 5.97–5.87 (m, 1H), 5.68 (d, J = 4.0 Hz, 1H), 5.11 (dd, J = 17.2 Hz, 1.2 Hz, 1H), 5.06 (d, J = 10.0 Hz, 1H), 4.52 (t, J = 4.0 Hz, 1H), 4.02 (dd, J = 7.8 Hz, 4.8 Hz, 1H), 3.81–3.70 (m, 1H), 3.73 (t, J = 8.0 Hz, 1H), 2.54–2.50 (m, 1H), 2.33–2.26 (m, 1H), 1.55 (s, 3H), 1.36 (s, 3H), 1.13–1.04 (m, 28H); $^{13}C\{^1H\}$NMR (101 MHz, $CDCl_3$): δ 134.8, 117.5, 112.9, 103.2, 81.2, 81.0, 76.0, 75.6, 40.5, 27.4, 27.0, 18.1, 17.8, 17.8, 17.7, 17.5, 17.3, 17.2, 13.7, 13.3, 13.1, 13.0; HRMS (ESI-TOF) m/z: $[M + Na]^+$ calcd for $C_{23}H_{44}NaO_6Si_2$ 495.2574, found 495.2556.

Solid-phase oligonucleotide synthesis. The oligonucleotide synthesis was carried out with a DNA/RNA synthesizer by the phosphoramidite method. After the synthesis, the CPG beads were treated with 10% dimethylamine in acetonitrile (CH_3CN) for 5 min followed by a rinse with CH_3CN to selectively deprotect cyanoethyl groups. Then, the oligonucleotides were deprotected and cleaved from CPG beads by incubated in the mixture of concentrated NH_3 aqueous solution/40% methylamine (1 : 1, v/v) for 10 min at 65 °C. Next, 2′-*O*-TBDMS groups were deprotected by treatment with $Et_3N\cdot3HF$ (125 μL) in DMSO (100 μL) at 65 °C for 1.5 h. The reaction was quenched with 0.1 M TEAA buffer (pH 7.0), and the mixture was desalted by a Sep-Pak C18 cartridge. The impure oligomers were purified using denaturing 20% PAGE containing 7 M urea to give highly purified oligonucleotides.

MALDI-TOF/MS analysis of ONs. The spectra were retrieved with a matrix assisted laser desorption/ionization time-of-flight (MALDI-TOF) mass spectrometer equipped with a nitrogen laser (337 nm, 3 ns pulse). A mixture of 3-hydroxypicolinic acid (3-HPA) and diammonium hydrogen citrate in H_2O was used as the matrix. The data of synthetic oligonucleotides: RNA **1** m/z = 6504.12 (calcd for $C_{194}H_{244}N_{65}O_{150}P_{20}$ $[M-H]^-$, 6506.43); RNA **2** m/z = 6545.59 (calcd for $C_{197}H_{250}N_{65}O_{150}P_{20}$ $[M-H]^-$, 6548.52); RNA **3** m/z = 6718.21 (calcd for $C_{206}H_{271}N_{68}O_{150}P_{20}$ $[M-H]^-$, 6719.85); RNA **4** m/z = 6546.83 (calcd for $C_{197}H_{250}N_{65}O_{150}P_{20}$ $[M-H]^-$, 6548.52); RNA **5** m/z = 6717.47 (calcd for $C_{206}H_{271}N_{68}O_{150}P_{20}$ $[M-H]^-$, 6719.85); RNA **6** m/z = 6546.03 (calcd for $C_{197}H_{250}N_{65}O_{150}P_{20}$ $[M-H]^-$, 6548.52); RNA **7** m/z = 6718.32 (calcd for $C_{206}H_{271}N_{68}O_{150}P_{20}$ $[M-H]^-$, 6719.85); RNA **8** m/z = 6814.75 (calcd for $C_{203}H_{247}N86O_{144}P_{20}$ $[M-H]^-$, 6815.76); RNA **9** m/z = 6546.55 (calcd for $C_{197}H_{250}N_{65}O_{150}P_{20}$ $[M-H]^-$, 6548.52); RNA **10** m/z = 6718.28 (calcd for $C_{206}H_{271}N_{68}O_{150}P_{20}$ $[M-H]^-$, 6719.85); RNA **11** m/z = 6546.58 (calcd for $C_{197}H_{250}N_{65}O_{150}P_{20}$ $[M-H]^-$, 6548.52); RNA **12** m/z = 6717.51 (calcd for $C_{206}H_{271}N_{68}O_{150}P_{20}$ $[M-H]^-$, 6719.85); RNA **13** m/z = 6547.07 (calcd for $C_{197}H_{250}N_{65}O_{150}P_{20}$ $[M-H]^-$, 6548.52); RNA **14** m/z = 6717.66 (calcd for $C_{206}H_{271}N_{68}O_{150}P_{20}$ $[M-H]^-$, 6719.85); RNA **15** m/z = 6547.62 (calcd for $C_{197}H_{250}N_{65}O_{150}P_{20}$ $[M-H]^-$, 6548.52); RNA **16** m/z = 6720.78 (calcd for $C_{206}H_{271}N_{68}O_{150}P_{20}$ $[M-H]^-$, 6719.85); RNA **17** m/z = 6590.81 (calcd for $C_{200}H_{256}N_{65}O_{150}P_{20}$ $[M-H]^-$, 6590.61); RNA **18** m/z = 6932.71 (calcd for $C_{218}H_{298}N_{71}O_{150}P_{20}$ $[M-H]^-$, 6933.27); RNA **19** m/z = 6619.17 (calcd for $C_{202}H_{260}N_{65}O_{150}P_{20}$ $[M-H]^-$, 6618.67); RNA **20** m/z = 7076.39 (calcd for $C_{226}H_{316}N_{73}O_{150}P_{20}$ $[M-H]^-$, 7075.55); RNA **21** m/z = 6647.38 (calcd for $C_{204}H_{264}N_{65}O_{150}P_{20}$ $[M-H]^-$, 6646.73); RNA **22** m/z = 7218.06 (calcd for $C_{234}H_{334}N_{75}O_{150}P_{20}$ $[M-H]^-$, 7217.83); RNA **23** m/z = 6829.30 (calcd for $C_{204}H_{249}N_{86}O_{144}P_{20}$ $[M-H]^-$, 6829.79); RNA **24** m/z = 6886.14 (calcd for $C_{207}H_{256}N_{87}O_{144}P_{20}$ $[M-H]^-$, 6886.90); RNA **25** m/z = 6830.45 (calcd for $C_{204}H_{249}N_{86}O_{144}P_{20}$ $[M-H]^-$, 6829.79); RNA **26** m/z = 6885.07 (calcd for $C_{207}H_{256}N_{87}O_{144}P_{20}$ $[M-H]^-$, 6886.90); RNA **27** m/z = 6828.58 (calcd for $C_{204}H_{249}N_{86}O_{144}P_{20}$ $[M-H]^-$, 6829.79); RNA **28** m/z = 6883.91 (calcd for $C_{207}H_{256}N_{87}O_{144}P_{20}$ $[M-H]^-$, 6886.90); RNA **29** m/z = 6829.21 (calcd for $C_{204}H_{249}N_{86}O_{144}P_{20}$ $[M-H]^-$, 6829.79); RNA **30** m/z = 6885.63 (calcd for $C_{207}H_{256}N_{87}O_{144}P_{20}$ $[M-H]^-$, 6886.90); RNA **31** m/z = 6828.19 (calcd for $C_{204}H_{249}N_{86}O_{144}P_{20}$ $[M-H]^-$, 6829.79); RNA **32** m/z = 6885.74 (calcd for $C_{207}H_{256}N_{87}O_{144}P_{20}$ $[M-H]^-$, 6886.90); RNA **33** m/z = 6827.76 (calcd for $C_{204}H_{249}N_{86}O_{144}P_{20}$ $[M-H]^-$, 6829.79); RNA **34** m/z = 6885.46 (calcd for $C_{207}H_{256}N_{87}O_{144}P_{20}$ $[M-H]^-$, 6886.90); RNA **35** m/z = 6829.69 (calcd for $C_{204}H_{249}N_{86}O_{144}P_{20}$ $[M-H]^-$, 6829.79); RNA **36** m/z = 6886.34 (calcd for $C_{207}H_{256}N_{87}O_{144}P_{20}$ $[M-H]^-$, 6886.90); RNA **37** m/z = 6831.79 (calcd for $C_{204}H_{249}N_{86}O_{144}P_{20}$ $[M-H]^-$, 6829.79); RNA **38** m/z = 6886.96 (calcd for $C_{207}H_{256}N_{87}O_{144}P_{20}$ $[M-H]^-$, 6886.90); RNA **39** m/z = 7447.08 (calcd for $C_{232}H_{275}N_{87}O_{148}P_{21}FS_4$ $[M-H]^-$, 7448.71).

Dual-luciferase assay. HeLa cells were transfected with the psiCHECK-2 vector (Promega) and the pcDNA3.1 containing a hygromycin resistance gene (Thermo Fisher Scientific). HeLa Cells were grown in the presence of 0.5 mg mL^{-1} hygromycin for 1 week. Stable HeLa-psiCHECK-2 cells expressing both firefly and *Renilla* luciferases were grown in Dulbecco's Modified Eagle Medium (D-MEM) supplemented with 0.25 mg mL^{-1} hygromycin and 10% bovine serum (BS) at 37 °C. 24 hours prior to transfection of siRNAs, HeLa-psiCHECK-2 cells (8.0×10^4 mL^{-1}) were grown in a 96-well plate (100 μL per well). The cells were transfected with siRNAs targeting the *Renilla* luciferase gene using lipofectamine RNAiMAX in opti-MEM reduced serum medium. Transfection without siRNAs was used as a control. The cells were incubated for 1 hour, D-MEM (50 μL) containing 10% BS was added to each well and cells were further incubated for another 24 hours. The activities of firefly and *Renilla* luciferases in the cells were measured using the Dual-Luciferase Reporter Assay System (Promega) according to a manufacture's protocol. The activity of *Renilla* luciferase was normalized by the firefly luciferase activity. The results were confirmed by at least three independent transfection experiments with two cultures each and are expressed as the average from four experiments as mean ± SD.

Thermal stability of siRNA duplexes. The solution containing 3.0 μM passenger strand and guide strand of siRNA in a buffer of 10 mM sodium phosphate (pH 7.0) containing 100 mM NaCl was heated at 100 °C and then cooled gradually to room temperature and used for the UV melting experiment.

 © 2022 The Author(s). Published by the Royal Society of Chemistry

Thermally induced transitions were recorded at 260 nm with a UV/vis spectrometer fitted with temperature controller in quartz cuvettes with a path length of 1.0 cm. The sample temperature was increased by 0.5 °C min^{-1}.

Nuclease resistance of siRNA. Fluorescein labeled siRNAs (600 pmol) were dissolved in 20 μL of a buffer of 10 mM sodium phosphate (pH 7.0) containing 100 mM NaCl. The samples were hybridized by heating 100 °C and then cooling gradually to room temperature to use for the serum stability test. 45 μL of opti-MEM and 60 μL of bovine serum were added, and the solution was incubated at 37 °C for the required time. Aliquots of 6.7 μL were diluted with a stop solution (65 mM EDTA, 15% glycerol, 6.0 μL). Samples were subjected to electrophoresis in nondenaturing 15% polyacrylamide-TBE and analyzed by a Luminescent Image analyzer LAS-4000 (Fujifilm).

Quantitative reverse-transcriptional PCR (RT-qPCR) analysis. Human colon cancer HCT116 cells (2.0×10^5 mL^{-1}) were plated in a 12-well plate (1 mL per well) before transfection. The cells were transfected with siRNAs using Lipofectamine RNAiMAX. After a 24 h incubation, cells were replated in fresh cell culture media and were further incubated for another 24 hours. Then, total RNA of the cells was extracted using an NucleoSpin RNA Plus Kit (Takara Bio, Shiga, Japan). cDNA was synthesized using a PrimeScript RT Master Mix (Takara Bio) and qRT-PCR was performed using a TB Green Premix Ex Taq II (Takara Bio) with a Thermal Cycler Dice Real Time System (Takara Bio). Primer sequences were for human *ACTB*: forward 5′-GGAGCAATGATCTTGATCTT-3′, reverse 5′-CCTTCCTGGGCATGGAGTCCT-3′ and for human *KNTC2*: 5′-CCTCTCCATGCAGGAGTTAAGA-3′, reverse 5′-GGTCTCGGGTCCTTGATTTTCT-3′. All reactions were run in duplicate, and the relative expression levels were determined by the ΔΔCT method.

Conflicts of interest

There are no conflicts of interest to declare.

Acknowledgements

This work was supported by the Japan Agency for Medical Research and Development (AMED) through its Funding Program for the research project number: 21ae0121029h0001. This work was also supported by JST SPRING, grant number JPMJSP2125. The authors thank Professor Yoko Hirata (Gifu University) for supplying the cells and providing technical advice. The authors would like to thank Ms Miwa Kawade (GF Mille Co., Ltd) for donating the modified *KNTC2*-siRNA (siRNA **49**) containing (*S*)-5′-*C*-aminopropyl-2′-*O*-methyluridine. The authors also would like to thank Dr Yasuko Kohda (BIKAKEN) for her technical assistance.

References

1 A. Fire, S. Q. Xu, M. K. Montgomery, S. A. Kostas, S. E. Driver and C. C. Mello, Potent and specific genetic interference by double stranded RNA in Caenorhabditis elegans, *Nature*, 1998, **391**, 806–811.
2 S. M. Elbashir, J. Harborth, W. Lendeckel, A. Yalcin, K. Weber and T. Tuschl, Duplexes of 21 ± nucleotide RNAs mediate RNA interference in cultured mammalian cells, *Nature*, 2001, **411**, 494–498.
3 S. M. Elbashir, W. Lendeckel and T. Tuschl, RNA interference is mediated by 21-and 22-nucleotide RNAs, *Genes Dev.*, 2001, **15**, 188–200.
4 S. F. Dowdy, Overcoming cellular barriers for RNA therapeutics, *Nat. Biotechnol.*, 2017, **35**, 222–229.
5 K. Garber, Worth the RISC?, *Nat. Biotechnol.*, 2017, **35**, 198–202.
6 A. Khvorova and J. K. Watts, The chemical evolution of oligonucleotide therapies of clinical utility, *Nat. Biotechnol.*, 2017, **35**, 238–248.
7 T. C. Roberts, R. Langer and M. J. A. Wood, Advances in oligonucleotide drug delivery, *Nat. Rev. Drug Discovery*, 2020, **19**, 673–694.
8 S. Ly, D. M. Navaroli, M. C. Didiot, J. Cardia, L. Pandarinathan, J. F. Alterman, K. Fogarty, C. Standley, L. M. Lifshitz, K. D. Bellve, M. Prot, D. Echeverria, S. Corvera and A. Khvorova, Visualization of self-delivering hydrophobically modified siRNA cellular internalization, *Nucleic Acids Res.*, 2017, **45**, 15–25.
9 C. R. Allerson, N. Sioufi, R. Jarres, T. P. Prakash, N. Naik, A. Berdeja, L. Wanders, R. H. Griffey, E. E. Swayze and B. Bhat, Fully 2'-modified oligonucleotide duplexes with improved *in vitro* potency and stability compared to unmodified small interfering RNA, *J. Med. Chem.*, 2005, **48**, 901–904.
10 X. Shen and D. R. Corey, Chemistry, mechanism and clinical status of antisense oligonucleotides and duplex RNAs, *Nucleic Acids Res.*, 2018, **46**, 1584–1600.
11 S. Ly, D. Echeverria, J. Sousa and A. Khvorova, Single-stranded phosphorothioated regions enhance cellular uptake of cholesterol-conjugated siRNA but not silencing efficacy, *Mol. Ther.*, 2020, **21**, 991–1005.
12 D. J. Foster, C. R. Brown, S. Shaikh, C. Trapp, M. K. Schlegel, K. Qian, A. Sehgal, K. G. Rajeev, V. Jadhav, M. Manoharan, S. Kuchimanchi, M. A. Maier and S. Milstein, Advanced siRNA designs further improve *in vivo* performance of GalNAc-siRNA conjugates, *Mol. Ther.*, 2018, **26**, 708–717.
13 C. R. Brown, S. Gupta, J. Qin, T. Racie, G. He, S. Lentini, R. Malone, M. Yu, S. Matsuda, S. S. Morskaya, A. V. Nair, C. S. Theile, K. Schmidt, A. Shahraz, V. Goel, R. G. Parmar, I. Zlatev, M. K. Schlegel, J. K. Nair, M. Jayaraman, M. Manoharan, D. Brown, M. A. Maier and V. Jadhav, Investigating the pharmacodynamic durability of GalNAc–siRNA conjugates, *Nucleic Acids Res.*, 2020, **48**, 11827–11844.
14 E. Malek-Adamian, D. C. Guenther, S. Matsuda, S. Martínez-Montero, I. Zlatev, J. Harp, M. B. Patrascu, D. J. Foster, J. Fakhoury, L. Perkins, N. Moitessier, R. M. Manoharan, N. Taneja, A. Bisbe, K. Charisse, M. Maier, K. G. Rajeev, M. Egli, M. Manoharan and M. J. Damha, 4'-*C*-Methoxy-2'-deoxy-2'-fluoro modified ribonucleotides improve

© 2022 The Author(s). Published by the Royal Society of Chemistry

metabolic stability and elicit efficient RNAi-mediated gene silencing, *J. Am. Chem. Soc.*, 2017, **139**, 14542–14555.

15 E. Malek-Adamian, M. B. Patrascu, S. K. Jana, S. Martínez-Montero, N. Moitessier and M. J. Damha, Adjusting the structure of 2'-modified nucleosides and oligonucleotides *via* C4'-α-F or C4'-α-OMe substitution: synthesis and conformational analysis, *J. Org. Chem.*, 2018, **83**, 9839–9849.

16 J. M. Harp, D. C. Guenther, A. Bisbe, L. Perkins, S. Matsuda, G. R. Bommineni, I. Zlatev, D. J. Foster, N. Taneja, K. Charisse, M. A. Maier, K. G. Rajeev, M. Manoharan and M. Egli, Structural basis for the synergy of 4'- and 2'-modifications on siRNA nuclease resistance, thermal stability and RNAi activity, *Nucleic Acids Res.*, 2018, **46**, 8090–8104.

17 E. Malek-Adamian, J. Fakhoury, A. E. Arnold, S. Martínez-Montero, M. S. Shoichet and M. J. Damha, Effect of sugar 2', 4'-modifications on gene silencing activity of siRNA duplexes, *Nucleic Acid Ther.*, 2019, **29**, 187–194.

18 A. V. Kel'in, I. Zlatev, J. Harp, M. Jayaraman, A. Bisbe, J. O'Shea, N. Taneja, R. M. Manoharan, S. Khan, K. Charisse, M. A. Maier, M. Egli, K. G. Rajeev and M. Manoharan, Structural basis of duplex thermodynamic stability and enhanced nuclease resistance of '-*C*-methyl pyrimidine-modified oligonucleotides, *J. Org. Chem.*, 2016, **81**, 2261–2279.

19 A. Mikami, N. Erande, S. Matsuda, A. Kel'in, L. B. Woods, T. Chickering, P. S. Pallan, M. K. Schlegel, I. Zlatev, M. Egli and M. Manoharan, Synthesis, chirality-dependent conformational and biological properties of siRNAs containing 5'-(*R*)- and 5'-(*S*)-*C*-methyl-guanosine, *Nucleic Acids Res.*, 2020, **48**, 10101–10124.

20 R. Kajino, Y. Maeda, H. Yoshida, K. Yamagishi and Y. Ueno, Synthesis and biophysical characterization of RNAs containing (*R*)- and (*S*)-5'-*C*-aminopropyl-2'-*O*-methyluridines, *J. Org. Chem.*, 2019, **84**, 3388–3404.

21 R. Kajino and Y. Ueno, (*S*)-5'-*C*-Aminopropyl-2'-*O*-methyl nucleosides enhance antisense activity in cultured cells and binding affinity to complementary single-stranded RNA, *Bioorg. Med. Chem.*, 2021, **30**, 115925.

22 S. Knapp, M. R. Madduru, Z. Lu, G. J. Morriello, T. J. Emge and G. A. Doss, Synthesis of griseolic acid B by π-face-dependent radical cyclization, *Org. Lett.*, 2001, **3**, 3583–3585.

23 R. D. Giacometti, J. C. Salinas, M. E. Østergaard, E. E. Swayze, P. P. Seth and S. Hanessian, Design, synthesis, and duplex-stabilizing properties of conformationally constrained tricyclic analogues of LNA, *Org. Biomol. Chem.*, 2016, **14**, 2034–2040.

24 A. M. Sørensen, K. E. Nielsen, B. Vogg, J. P. Jacobsen and P. Nielsen, Synthesis and NMR-studies of dinucleotides with conformationally restricted cyclic phosphotriester linkages, *Tetrahedron*, 2001, **57**, 10191–10201.

25 Y. Zhou, R. Kajino, S. Ishii, K. Yamagishi and Y. Ueno, Synthesis and evaluation of (*S*)-5'-*C*-aminopropyl and (*S*)-5'-*C*-aminopropyl-2'-arabinofluoro modified DNA oligomers for novel RNase H-dependent antisense oligonucleotides, *RSC Adv.*, 2020, **10**, 41901–41914.

26 S. Furegati, A. J. P. White and A. D. Miller, Observation of a 1,5-silyl-migraftion on fructose, *Synlett*, 2005, **15**, 2385–2387.

27 M. Govindarajan, Protecting group migrations in carbohydrate chemistry, *Carbohydr. Res.*, 2020, **497**, 108151.

28 S. De, S. D. Jonghe and P. Herdewijn, Synthesis of a 3'-fluoro-3'-deoxytetrose adenine phosphonate, *J. Org. Chem.*, 2017, **82**, 9464–9478.

29 V. Korotkovs, L. F. Reichenbach, C. Pescheteau, G. A. Burley and R. M. J. Liskamp, Molecular construction of sulfonamide antisense oligonucleotides, *J. Org. Chem.*, 2019, **84**, 10635–10648.

30 H. Blade, D. Bradley, L. Diorazio, T. Evans, B. R. Hayter and G. P. Howell, Modular Synthesis of constrained ethyl (cEt) purine and pyrimidine nucleosides, *J. Org. Chem.*, 2015, **80**, 5337–5343.

31 T. A. Rand, S. Petersen, F. Du and X. Wang, Argonaute2 cleaves the anti-guide strand of siRNA during RISC activation, *Cell*, 2005, **123**, 621–629.

32 J. J. Song, S. K. Smith, G. J. Hannon and L. Joshua-Tor, Crystal structure of argonaute and its implications for RISC slicer activity, *Science*, 2004, **305**, 1434–1437.

33 S. Harikrishna and P. I. Pradeepkumar, Probing the binding interactions between chemically modified siRNAs and human Argonaute 2 using microsecond molecular dynamics simulations, *J. Chem. Inf. Model.*, 2017, **57**, 883–896.

34 J. J. Turner, S. W. Jones, S. A. Moschos, M. A. Lindsay and M. J. Gait, MALDI-TOF mass spectral analysis of siRNA degradation in serum confirms an RNAse A-like activity, *Mol. BioSyst.*, 2007, **3**, 43–50.

35 N. Kaneko, K. Miura, Z. Gu, H. Karasawa, S. Ohnuma, H. Sasaki, N. Tsukamoto, S. Yokoyama, A. Yamamura, H. Nagase, C. Shibata, I. Sasaki and A. Horii, siRNA-mediated knockdown against CDCA1 and KNTC2, both frequently overexpressed in colorectal and gastric cancers, suppresses cell proliferation and induces apoptosis, *Biochem. Biophys. Res. Commun.*, 2009, **390**, 1235–1240.

36 Y. Makita, S. Murata, Y. Katou, K. Kikuchi, H. Uejima, M. Teratani, Y. Hoashi, E. Kenjo, S. Matsumoto, M. Nogami, K. Otake and Y. Kawamata, Anti-tumor activity of KNTC2 siRNA in orthotopic tumor model mice of hepatocellular carcinoma, *Biochem. Biophys. Res. Commun.*, 2017, **493**, 800–806.

© 2022 The Author(s). Published by the Royal Society of Chemistry